

NACA RM E53I15

6839

TECH LIBRARY KAFB, NM
0143280

NACA

RESEARCH MEMORANDUM

ANALYSIS OF PART-SPEED OPERATION FOR HIGH-PRESSURE-RATIO
MULTISTAGE AXIAL-FLOW COMPRESSORS

By William A. Benser

Lewis Flight Propulsion Laboratory
Cleveland, Ohio

Classification cancelled (or changed to *UNCLASSIFIED*)
By Authority of *NASA Tech. Pub. Administration #07*
(OFFICER AUTHORIZED TO CHANGE)

By *WAB*
NAME

GRADE OF OFFICER MAKING CHANGE)

4 Apr 61
DATE

CLASSIFIED DOCUMENT

**NATIONAL ADVISORY COMMITTEE
FOR AERONAUTICS**

WASHINGTON

December 4, 1953

**RECEIPT SIGNATURE
REQUIRED**

CONFIDENTIAL



0143280

NACA RM E53115

NATIONAL ADVISORY COMMITTEE FOR AERONAUTICS

RESEARCH MEMORANDUMANALYSIS OF PART-SPEED OPERATION FOR HIGH-PRESSURE-RATIO
MULTISTAGE AXIAL-FLOW COMPRESSORS

By William A. Benser

SUMMARY

An analysis of the part-speed operation problems of high-pressure-ratio multistage axial-flow compressors was made by means of a stage-stacking technique. This analysis indicated that either discontinuities in the performance of inlet stages or stage interactions could result in multiple over-all compressor performance characteristic curves at a given speed in the intermediate-speed range. The particular performance curve obtained at a given speed depends on the manner of throttling and speed change used in setting the compressor operating points. The dip in the surge characteristics, frequently obtained in component tests of high-pressure-ratio multistage axial-flow compressors, is most likely a discontinuous change from the surge limit for operation with the inlet stalled to operation with the inlet unstalled.

Inasmuch as multiple performance curves do exist in the intermediate-speed range, the surge limit obtained by variation of throttle setting at a constant speed may not represent the actual limit to operation in this speed range. Additional usable operating conditions may be obtained by variation of testing technique, such as variation of speed at a fixed throttle setting. Thus, the intermediate-speed surge limit obtained in engine operation may not be the same as that obtained by conventional compressor-component rating techniques.

Extremely low part-speed efficiencies of high-pressure-ratio compressors may to a large extent be attributed to severe stall characteristics of inlet stages or stage interactions or both. Stages with continuous performance characteristics at their stall points ("soft-stall" stages) when operated in a multistage compressor are desirable from the standpoint of good part-speed efficiency and surge-limit characteristics.

The results of this analysis are in general agreement with experimental observations in tests of high-pressure-ratio multistage axial-flow compressors.

3024

T T C

INTRODUCTION

High-pressure-ratio multistage axial-flow compressors generally exhibit low efficiencies at part speed, and component tests indicate a sharp dip or kink in the surge line at intermediate rotational speeds. In the application of this type compressor to turbojet engines for aircraft, auxiliary means such as adjustable guide vanes or air bleed have been required in order to obtain satisfactory acceleration and to avoid encountering surge at intermediate speeds. From the standpoint of engine weight and simplicity, therefore, it is desirable to improve low-speed performance and to minimize or, if possible, to eliminate the dip in the surge limit. Accomplishment of these objectives, however, requires an understanding of the flow processes at low and intermediate speeds.

Inasmuch as both poor low-speed performance and compressor surge in multistage axial-flow compressors are due to stalling of one or more stages of the compressor, some insight into these part-speed operating problems may be obtained from consideration of stage stall characteristics. Recent studies have shown that in most cases stage stall results in the formation of one or more low-flow or stalled zones rather than a uniform stall of all blades (refs. 1 to 4). These stall zones rotate about the compressor axis, and thus this type of stall is designated as rotating stall. From the detailed interstage survey data for a 16-stage axial-flow compressor (ref. 5), it was concluded that the dip in the surge limit was a result of stage interactions or deterioration of the performance of several stages due to stall of the first stage. Reference 6 indicated that the type of rotating stall occurring in the inlet stages of a multistage compressor may also be a pertinent factor in the determination of part-speed surge characteristics. This reference also showed that a compressor may surge or may stall completely, depending on the compressor, throttle, and external system characteristics. Inasmuch as either surge or complete compressor stall occurs at the same operating condition, this lower limit of operation at any speed is referred to as surge in this report in order to avoid confusion between complete compressor stall and individual stage stall.

As shown in reference 2, when either rotating stall or surge exists in a multistage axial-flow compressor, the flow disturbances extend completely through the compressor from entrance to exit. Thus, experimental determination of the stage or group of stages that instigated the rotating stall or surge is not always possible. Because of interaction effects, the individual stage performance and stall characteristics of a component of a multistage compressor may be appreciably different from those obtained in single-stage tests. Interaction effects are defined as the effects of radial maldistribution of flow imposed by adjacent stages and the effects of nonsteady flow resulting from rotating stall originating in adjacent stages. Some insight into the effects of type of stage stall and of stage interactions on the part-speed performance problem may

be obtained by a simple stage-stacking analysis in which these effects are approximated in the characteristics of the individual stages.

For the analysis reported herein, the same hypothetical 12-stage compressor discussed in reference 6 was chosen, and the effects of inlet-stage stall characteristics and stage interactions were estimated by arbitrary adjustment of the stalled characteristics of the individual stages. The main objective of this analysis is to study the intermediate-speed surge problem. Some evaluation of the poor low-speed performance problem is also obtained. In addition, a hysteresis effect in the unstalling of the inlet stage has been considered. Because of the simplifying assumptions made in regards to stage performance characteristics and Mach number effects, the computed values of multistage performance can be considered only as qualitative. The general trends, however, are valuable in obtaining an understanding of the off-design performance problems for high-pressure-ratio multistage axial-flow compressors.

SINGLE-STAGE STALL CHARACTERISTICS

Recent hot-wire anemometer studies of stalling characteristics of axial-flow compressor stages have shown that, in the majority of cases, stage stall is not a uniform stall of all blades but consists of stalled zones, which rotate about the compressor axis (refs. 1, 3, and 4). These stall zones divide the flow into two categories: a low-flow or stalled region and a high-flow or unstalled region. This redistribution of flow reduces the angles of attack and therefore the tendency for stall in the high-flow region. The radial depth of the stalled or low-flow zones are apparently dependent on the rate at which each radial element approaches its stalling angle of attack as compressor weight flow is reduced. This rate of approach to stall is, in turn, dependent on the radial variation of inlet conditions as well as the radial variation of such blade geometry parameters as solidity and camber. Thus, there is a wide variation of stall patterns for different stage designs. Variations of inlet conditions may also result in variations of stall pattern for any given stage design. In general, however, as stated in reference 2, rotating stall may be divided into two general types: (1) progressive or partial-span stall, and (2) root-to-tip or total-span stall. Partial-span stall is characterized by stall zones that occur over only a portion of the blade span; whereas for total-span stall, the stall zone covers the entire blade span.

Partial-span stall. - Partial-span stall occurs in stages where one end of the blade approaches a stalling angle of attack at an appreciably higher compressor flow than does the other end. Thus, this type of stall is prevalent in low hub-tip ratio or inlet-type stages, where large variations of rate of change of angle of attack with weight flow exist from root to tip. Representative performance curves for a stage having a

3024
CM-T back

partial-span type of rotating stall are given in figure 1(a) as a plot of adiabatic efficiency η and pressure coefficient ψ against flow coefficient Φ . Both the pressure coefficient and efficiency curves are continuous functions of flow coefficient and decrease gradually as flow is decreased below the value for stall (point A, fig. 1(a)). This type of characteristic has been obtained for a number of inlet-type single-stage compressors (refs. 1 and 7 to 9). Rotating-stall data, however, were not taken in all these investigations.

Shown on figure 1(b) is a cross-sectional sketch of a typical partial-span stall pattern in which the shaded areas designate the low-flow or stalled zones. These stall zones, which are usually concentrated near the blade tips, rotate in the direction of rotor rotation with respect to an absolute frame of reference, but generally at an appreciably lower speed than the rotor. Thus, this represents a counterrotation relative to the rotor. Tip stall patterns having from one to eight stall zones have been observed.

Variations in stage geometry or inlet-velocity distributions may result in partial-span stall patterns somewhat different from that shown in figure 1(b). For example, stages may operate with conditions that are more critical at the hub than at the tip and may have a stall originating at the blade root. Or, if the operation of the tip section is extremely critical compared with that of radial sections a short distance in from the tip, the tip stall may be broad circumferentially and shallow in the radial direction as indicated in figure 1(c). In fact, tip stall may be uniform from blade to blade and no rotating stall would exist at the tip region, but the resultant stage characteristics would not differ appreciably from those shown in figure 1(a).

In general, inlet-type stages exhibit a partial-span-type tip stall. Thus, the stage characteristics presented in figure 1(a) may be considered as representative of those for the inlet stages of high-performance jet-engine compressors.

Total-span stall. - Axial-flow compressor stages in which stalling angle of attack is approached simultaneously at all radii have rotating stall designated as the total-span type. From tests of single-stage units, it has been shown that this type stall is generally associated with high hub-tip ratio stages, 0.8 or over, and in most cases a sharp drop in pressure coefficient results from the occurrence of stall. A typical performance curve for a stage having this type stall is presented in figure 2(a). Rotating stall occurs at point A, and, when stall occurs, the pressure coefficient drops to about two-thirds of the value prior to stall. Changes in flow following stall result in operation on the lower or dashed portion of the characteristic curve. In order to effect stall recovery, the flow coefficient must be increased somewhat above the initial value for instigation of stall; thus, a hysteresis

effect exists. The variations in stage efficiency follow the same general trend. Figure 2(b) shows a cross-sectional sketch of the stalled zone. This stall generally consists of a single zone that covers an appreciable part of the annulus and rotates at a much lower speed than the rotor.

The intermediate and high hub-tip ratio stages discussed in references 1 and 4 exhibited the general type performance characteristic shown in figure 2(a) when total-span stall occurred. The 0.76 hub-tip ratio stage reported in reference 10, however, showed no discontinuity in performance at the point of instigation of total-span stall. Stages that are equally critical over all or a major part of the blade span, however, may be expected to exhibit a sharp drop in pressure coefficient at the stall point. Two distinct performance curves with unstalling hysteresis similar to that shown in figure 2(a) are then apt to occur.

Combinations of partial-span- and total-span-type stall. - As pointed out previously, rotating stall or stage stall occurs in a wide variety of forms depending on inlet flow conditions and blading geometry, and it is possible to have both partial-span- and total-span-type stall in a given stage, as discussed in references 1, 4, and 10. For the purpose of illustration, the curve for pressure coefficient against flow coefficient for the 0.8 hub-tip ratio stage discussed in reference 1 is presented in figure 3. Partial-span stall at the blade tip was obtained for a range of flow coefficients between points A and B. At point B the stall changed abruptly to a total-span type. This change in stall type resulted in a drop in pressure coefficient as shown and a hysteresis effect with total-span stall on the lower curve. For intermediate hub-tip ratio stages, therefore, a partial-span stall may be expected at the initial stall point and a transition to total-span stall at some lower value of flow coefficient.

Modified partial-span stall. - For low hub-tip ratio stages in which critical conditions are approached simultaneously over an appreciable part of the blade span, the initial stall pattern may be concentrated at one end of the blade but result in a discontinuity in stage performance similar to that for a total-span-type stall. In this case, however, the magnitude of drop in performance may be somewhat smaller than that indicated in figures 2(a) and 3(a). This type of stage stall is designated as a modified partial-span stall.

STAGE INTERACTIONS

The performance characteristics and stalling characteristics of a stage may be appreciably different when operated as a single stage from those when operated as a stage of a multistage compressor. These differences of performance may be designated as interaction effects and can be attributed to two main sources: (1) radial maldistribution of flow due to off-design performance of adjacent stages, and (2) nonsteady flow due to rotating stall originating in adjacent stages.

Radial maldistribution of flow. - Radial maldistribution of flow, defined as large variations from the design flow distribution, results from off-design performance of preceding stages. For example, as the flow coefficient of the first stage is decreased, the energy addition at the tip of this stage may increase more rapidly than that at the root. Consideration of radial equilibrium of static pressure at the discharge of the first stage leads to a ratio of axial velocity at the blade tip to axial velocity at the root that is larger than the design value. This radial variation from design flow may be aggravated through the first several stages of the compressor and may alter the relative rate of approach to stall for the tip and root sections of a given stage. For this example, critical conditions at the root and tip may be reached simultaneously for some stage farther back in the compressor. Thus, the stall pattern and performance characteristics of stages in a multistage compressor may be appreciably different from those predicted by single-stage tests.

Nonsteady flow. - When rotating stall exists in a multistage compressor, it extends through all the stages (ref. 2). Imposition of the flow fluctuations of rotating stall on any given stage that is operating near its stall point may result in stall of that stage. Thus, the flow fluctuations may be increased in magnitude. In addition to premature incurrence of stall in a given stage due to stall of an adjacent stage, the resulting stall pattern in the given stage may be appreciably different from that obtained in single-stage tests of that stage.

Stages that are operating near their choke limit, however, tend to decrease the amplitudes of flow fluctuation resulting from rotating stall.

STAGE STACKING

An approximation of the operating condition of each stage of a multistage compressor can be obtained for a wide range of speed and weight flow by a one-dimensional stage-stacking technique based on stage performance characteristics. The stacking technique used in this report is given in appendix B; it is assumed that the nondimensional stage performance, in terms of adiabatic efficiency and pressure coefficient, is represented as a function of flow coefficient, which is defined as the ratio of inlet axial velocity to wheel speed at the mean radius, and of the operating characteristics of preceding stages. Comparison of numerous stages on the basis of these parameters has given good correlation for relative stage-inlet Mach numbers up to approximately 0.75.

The main purpose of this analysis is to show qualitatively the effects of various stage-stall characteristics and stage interactions on the part-speed characteristics of high-pressure-ratio axial-flow compressors. Therefore, the stacking analysis outlined in appendix B was considered adequate, even though it did not account for effects of Mach number on stage range and efficiency. Mach number effects could be incorporated by interpolation of performance curves for

each stage, but this complication was not deemed necessary in this investigation. Interaction effects due to radial maldistribution of flow and interaction effects due to nonsteady flow resulting from rotating stall in the inlet stage were estimated by arbitrarily altering the individual stage performance curves of several succeeding stages for those conditions where rotating stall existed in the inlet stage. Estimated hysteresis effects in the unstalling characteristics were also incorporated in the stage curves. For the analysis reported herein, three combinations of stage stall, interaction effects, and unstalling hysteresis were considered.

Hypothetical compressor design. - The basic hypothetical compressor design was identical for all three cases considered and was the same as that presented in reference 6. The compressor had 12 stages of constant tip diameter. All stages had identical performance in terms of pressure coefficient and efficiency against flow coefficient except for the stalling characteristics. Other pertinent details on the design are as follows:

Over-all total-pressure ratio.	7.75
Inlet specific weight flow, $\frac{W\sqrt{\theta_1}}{\delta_1 A_1}$	33.5
Inlet corrected tip speed, ft/sec.	950
Absolute inlet-air angle at pitch radius of each stage, deg	$22\frac{1}{2}$
Reference-point flow coefficient for each stage.	0.69
Reference-point pressure coefficient for each stage.	0.3

A tabulation of the individual stage hub-tip ratios, area ratios, mean radius ratios, and reference-point pressure ratios is given in table I.

Cases analyzed. - The assumptions of stall type, interactions, and hysteresis effects for the three cases considered are as follows:

Case	Type of stall			Interactions	Hysteresis effects
	Stages 1 to 4	Stages 5 to 8	Stages 9 to 12		
I	Partial span	Partial span plus total span	Total span	None	None
II	Modified partial span	Partial span plus total span	Total span	Stages 2 to 4	Stage 1
III	Modified partial span	Partial span plus total span	Total span	Stages 2 to 8	Stage 1

~~CONFIDENTIAL~~

The individual stage curves assumed for each configuration are discussed in the section RESULTS.

Range of calculations. - For each case considered, calculations were made for a range of speed of 50 to 110 percent of the reference value. The maximum flow considered at each speed was the estimated exit-vane choke flow - a value of $W\sqrt{\theta}/\delta A$ equal to 41.4 pounds per second per square foot of annulus area at the exit of the twelfth stage. The minimum flow considered at each speed was that at which a discontinuity in the performance curve of any stage was encountered. As indicated in references 1 and 6, discontinuities in multistage compressor performance at a given speed may lead to either compressor surge or complete compressor stall. For simplicity these discontinuity points will be referred to as the compressor surge limit. Whether surge or complete compressor stall occurs, this discontinuity in compressor performance represents the lower limit of flow at any speed consistent with usable operation of the compressor. In the computation of intermediate-speed performance for cases II and III, operations with the inlet stage stalled and with the inlet stage unstalled were considered.

RESULTS

The computed performance results obtained in this analysis are presented in terms of over-all total-pressure ratio against inlet specific weight flow, that is, equivalent weight flow per square foot of annulus area. The pressure ratio presented is the total-pressure ratio to the exit of the twelfth stage and does not include an exit vane or diffuser loss. Computed efficiency contours are also shown on the performance maps. Because of the assumptions made in regard to stage performance characteristics and because Mach number effects were neglected, the results of this analysis are only qualitative. The general trends obtained, particularly in regard to the intermediate-speed surge problem, are, however, valuable in gaining an understanding of this phenomenon.

Case I

The assumed stage performance curves for case I are presented in figure 4. The first four stages were assumed to have only a partial-span stall, and the pressure coefficient and efficiency were taken as continuous functions of the flow coefficient as shown in figure 4(a). Stages 5 to 8 were assumed to have an initial partial-span stall and a total-span stall at lower values of flow coefficient (fig. 4(b)). Stages 9 to 12 were assumed to have only a total-span stall (fig. 4(c)). A discontinuity of stage characteristics was considered to exist when total-span stall occurred. The stage characteristics for stage pressure ratios below 1.00

~~CONFIDENTIAL~~

were the same for all stages (fig. 5). As noted in appendix B, a modified computational procedure was used when stages operated at turbinizing pressure ratios. Interaction effects were considered negligible throughout the compressor.

Computed over-all performance for case I. - The computed over-all performance map for case I is given in figure 6 as a plot of over-all total-pressure ratio against specific weight flow. Also shown on this figure are contours of constant efficiency, the choking-flow condition for the exit vanes, and the estimated surge limit. The surge limit was taken as the line through the discontinuity points at each speed. This surge limit does not exhibit the customary dip or kink at intermediate speeds. If surge had been assumed to occur at the maximum pressure-ratio points as was done in reference 11, the general trends would be unchanged.

Variation of stage flow coefficients. - In order to illustrate the stages that are stalled at various inlet flows and speeds, the stage flow coefficient has been plotted against stage number (fig. 7) for several values of inlet flow at speeds of 100, 80, and 50 percent of the reference value. The lightly shaded area on these plots represents the range of partial-span stall, and the heavily shaded area represents the range of total-span stall with the associated discontinuity of stage pressure coefficient (fig. 4).

At 100 percent of reference speed (fig. 7(a)), flow-coefficient variations are shown for the reference point $W\sqrt{\theta_1}/\delta_1 A_1 = 33.5$, the approximate exit-vane choke flow of 33.68, and the surge flow of 33.06. The variation of flow coefficient in the front stages is small, and thus the specific weight-flow range at this speed is also small. The maximum change in flow coefficient occurs in the last stage, and surge results from total-span stall of this stage.

As the speed is reduced to 80 percent of the reference value, the flow coefficients decrease for the entrance stage and increase for the exit stage as shown in figure 7(b). At this speed, the first stage operates in the partial-span stall range even at the maximum specific weight flow of 23.40. Surge results from total-span stall of the ninth stage at a specific weight flow of 17.16. It should also be noted that the number of stages operating in the partial-span stall range increases from one to eight as the flow is decreased from the exit-vane choke value of 23.40 to the surge value of 17.16.

As the speed is further decreased to 50 percent of the reference value (fig. 7(c)), the front stages move deeper into stall and the rear stages closer to choking flow. Surge results from occurrence of total-span stall in the fifth stage. From five to seven stages operate in the partial-span stall range at all flows.

Thus, from a comparison of figures 7(a), (b), and (c), it can be seen that at high speeds surge results from total-span stall of the rear stages, and, as speed is reduced, earlier stages in the compressor instigate surge. Because of the stage grouping and stage characteristics selected for this analysis, surge will only be instigated by stages 5, 9, and 12. To define more clearly the relation of stage stall to compressor speed and flow, the individual stage stall limits have been cross-plotted on the computed performance map in figure 8. This figure shows that partial span or tip stall exists in from one to eight stages over the complete flow range for all speeds below 80 percent of the reference value and for the low-flow portion of the flow range at speeds of 85 and 90 percent. This is consistent with the results of the stall studies of reference 2, except that the stall occurs at higher speeds. As was pointed out in reference 11, however, the speed at which inlet-stage stall first occurs can be varied by stage matching. For the example reported herein, no compromise was made in matching to improve low-speed performance. All stages were matched at the same value of flow coefficient at the reference point. It should be noted that, near the surge point at 90 percent speed, nearly all the stages are approaching stall simultaneously, and stages 2 to 5 stall at a slightly higher value of specific inlet flow than stage 1. The lines of total-span stall (fig. 8) show that, for speeds through 70 percent of the reference value, surge results from total-span stall of the fifth stage; for speeds of 75 through 90 percent, from total-span stall of the ninth stage; and for speeds of 95 percent and higher, from total-span stall of the twelfth stage. The resultant surge limit, however, is free of the normal dip or kink.

Case II

The study of reference 2 has indicated that rotating stall originating in a front stage may extend completely through the compressor. Therefore, the low-flow zones resulting from stall of an inlet stage will cause succeeding stages that are operating near their stall points to also stall. At intermediate and low speeds, the amplitude of flow fluctuations due to rotating stall of the inlet stage will be maintained through the first few stages, and the stage performance of these early stages will be reduced from that for steady inlet flow. Thus, these stage interactions must be considered in analysis of the part-speed compressor surge problem. Discontinuities in the first stage performance characteristic and unstalling hysteresis may also affect this problem. Therefore, case II was studied to evaluate the effects of a small discontinuity at the stall point and of an unstalling hysteresis on the performance of the inlet stage. In addition, interaction effects were assumed to result in a deterioration of the performance of stages 1 to 4, whenever stall existed in any of these stages. Inasmuch as the investigation of reference 2 indicated that the flow fluctuations of rotating

stall increased through the first four stages of a 10-stage compressor, the inclusion of interaction effects in the first four stages of this hypothetical compressor was believed to be a realistic assumption.

The stage curves for stages 1 to 4 were obtained by arbitrarily modifying the pressure-coefficient characteristics around the stall point from those used in case I and computing the modified efficiency curves, with an assumption of no change in temperature rise. The pressure-coefficient characteristics and resultant efficiency variations with flow coefficient for stages 1 to 4 are given in figure 9. As can be seen from a comparison of figure 9(a) with figures 4(b) and (c), the discontinuity assumed is much smaller than that anticipated from occurrence of total-span stall. Therefore, this may be assumed to be representative of the modified partial-span-type stall. The magnitude of decrease in pressure coefficient as a result of interactions in stages 2 to 4 (fig. 9(b)) was comparable to that assumed for stage 1. To evaluate interaction effects, stages 1 to 4 were assumed to operate on the lower or stalled portions of their performance curves whenever any of these stages encountered stall.

Calculations for this case were made for operation with the first four stages unstalled and for operation with the inlet stage stalled and interactions in stages 2 to 4.

Performance with front stage unstalled. - The calculated performance map for the unstalled condition of the inlet stages is presented in figure 10(a). As can be seen from this figure, surge at speeds of 95, 100, and 110 percent of the reference value results from stall of the twelfth stage, whereas surge for speeds of 80, 85, and 90 percent of the reference value results from stall of one of the first four stages. No operation with the front stage unstalled is obtainable below 80 percent speed. This performance map (fig. 10(a)) is identical to the high-speed part of the map for case I (figs. 6 and 8) except for the surge limit at speeds below 95 percent of the reference value. For speeds of 80 through 90 percent of the reference value, the discontinuity resulting in surge is caused by stall of one of the first stages and the associated interaction effects.

Performance with first stage stalled. - The computed performance for the condition of stall in the first stage and interactions in stages 2 to 4 is shown in figure 10(b) for speeds of 50 to 95 percent of the reference speed. The upper limit of flow for speeds of 85, 90, and 95 percent of the reference value was determined by the unstalling flow coefficient for the first stage. At 95 percent speed, the line of front-stage unstalling intersects the ninth-stage stall-limit line (fig. 10(b)). Therefore, this was the maximum speed for which calculations of performance with the front stage stalled were made. Surge at speeds of 50 through 70 percent results from discontinuities due to the occurrence of total-span stall of the fifth stage, and at speeds of 75 to 95 percent, from stall of the ninth stage. Other variations in stage characteristics than

those assumed might cause variations in the surge limit of figure 10(b), such that lower surge pressure ratios might be obtained at speeds of 75 to 95 percent speed. The efficiencies for case II at intermediate speeds are somewhat lower than for case I.

Complete performance map. - The complete performance map for case II is obtained by superimposing the performance maps with the inlet stage unstalled and the performance map with the inlet stage stalled and interactions in stages 2 to 4 (figs. 10(a) and (b)). The resultant performance in terms of pressure ratio against specific weight flow is given in figure 10(c) for a range of speeds from 50 to 110 percent of the reference value. From this figure it can be seen that for a range of speed from 80 to 95 percent of the reference value, operation with both the inlet stage stalled and the inlet stage unstalled is possible. Thus, in this intermediate-speed range, the existence of double performance curves and two surge points at a given speed is indicated. Whereas the double curves of this analysis were obtained as a result of a small discontinuity in the performance characteristics of the first stage and interactions in stages 2 to 4, similar results would have been obtained by any combination of simultaneous discontinuities of the front stages.

Triple-valued performance curves have been encountered experimentally (ref. 12), and unreported experiments have shown multiple-valued surge points for each of two relatively high-pressure-ratio commercial compressors operating at approximately 80 percent of design speed. In these tests, the particular surge point obtained depended upon the schedule of speed and flow, which preceded the occurrence of surge. The double-valued curves of figure 10(c) and the dependence of compressor performance on the manner in which a particular operating point is approached indicate the necessity of studying the transition from compressor operation with the inlet stage stalled to operation with the inlet stage unstalled.

Transition from stalled to unstalled operation of inlet stage. - The usual operation schedule in compressor component testing is to start at maximum or choke flow for a given speed and increase the throttling in successive steps until surge is obtained. Inasmuch as compressor operation at maximum flow at low and intermediate speeds is normally set by the choke of exit vanes, transition from stalled to unstalled operation of the inlet stage can be considered to occur at maximum flow or along the exit-vane choke limit of figure 10(c). Thus, as the compressor speed is increased, the choking limit of the exit vanes prevents unstalling of the inlet stages for this case until a speed of 85 percent of the reference value is attained. Unstalling of the inlet stage and alleviation of the resultant interaction effects result in a transient change of operation from the exit-vane choke point on the dashed curve to the exit-vane choke point on the solid curve. For this example, the specific weight flow increases from 26 to 26.3 and the pressure ratio from 4.23 to 4.30. The efficiency is not changed appreciably. For the purposes of

this report, the compressor operation is assumed to jump discontinuously, and transient conditions following unstalling of the inlet stage have not been considered.

The over-all performance map, anticipated from the normal compressor-component-rating techniques described previously, is given in figure 10(d). For speeds up to 85 percent of the reference value, the compressor would operate with the front stage stalled, and, for speeds above 85 percent, with the front stage unstalled. Therefore, both branches of the performance curve are given at the cross-over speed of 85 percent of the reference value.

Surge limit. - The surge limit (fig. 10(d)) will follow the discontinuity points of the dashed curves up to the cross-over speed and the discontinuity points on the solid curves above this speed. Thus, a surge line faired through these points exhibits the dip that is common to most high-pressure-ratio axial-flow compressors. As indicated by the analysis, this dip actually constitutes a discontinuity in the surge line, which results from transition of modes of operation of the compressor. Other variations of surge characteristics for the condition of front stage stalled may actually indicate a dip in the combined surge characteristic rather than the continuous variation shown on figure 10(c). In the presentation of experimental data, however, the surge line is faired through a finite number of points and has generally been considered a continuous function of flow, pressure ratio, and speed.

The analysis of case II therefore shows that the dip in the surge line is more likely a result of a discontinuity in the performance at the stall point of the first stage and of interactions in a few succeeding stages. Inasmuch as both factors result in sharp decreases in performance of the complete compressor, it is evident that either of these results could cause a dip or discontinuity in the surge limit at intermediate speeds. The transition from the surge limit for the inlet stage stalled to that for the inlet unstalled is dependent on the manner in which the surge condition is approached. If the compressor-discharge throttling is sufficient to cause the compressor to operate appreciably above the exit-vane choke limit as speed is increased, unstalling of the front stage may not be achieved until a speed of appreciably greater than 85 percent of the reference value is attained. In the range of speeds from 85 to 95 percent of the reference value, the surging limit may follow that of figure 10(b); whereas, if the speed is first increased above the value for unstalling of the inlet stage and then reduced, surging may occur on the surge line of figure 10(a) for speeds of 80 to 85 percent of the reference value. Thus, for case II, double-valued surge points at a given speed may be obtained for the range of speeds from 80 to 95 percent of reference speed, as indicated on figure 10(c). As previously discussed, this phenomenon has been observed in experimental studies of multistage axial-flow compressor performance. For cases where unstalling of groups of stages or

alleviation of interaction effects occurs stepwise, even more than two surge points may be obtained.

For maximum engine acceleration, the compressor operating line in an engine will be very close to the surge limit at low and intermediate speeds. Thus, the intermediate-speed surge limit obtained by normal compressor-rating techniques may not be representative of the compressor stall or surge limit, which is obtained during engine acceleration. Therefore, when multiple operating curves exist at any compressor speed, performance evaluations must include all possible operating conditions. This may be done by approaching a given operating point by variation of compressor speed at each of several fixed throttle settings, as well as by variation of throttle settings at a fixed speed. Speed changes must include both increases and decreases in rotative speed. An operating technique such as this will give performance maps of the type shown in figure 10(c) for those cases where multiple performance curves exist for a given compressor rotative speed.

Effect of unstalling hysteresis. - For case II, a hysteresis effect was assumed in the unstalling characteristics of the inlet stage. Hysteresis had no effect on the general trend of surge characteristics, except on the speed at which transition from stalled to unstalled operation of the inlet stage was achieved. With no hysteresis, unstalling of the inlet stage along the exit-vane choke line (fig. 10(b)) would be achieved at 81.5 percent of reference speed rather than at 85 percent, as for the case with hysteresis. Possible discontinuities in the surge limit and the potential of double-valued surge points between speeds of 80 to 93 percent can be seen from figure 10(c).

Part-speed efficiency. - Because of the manner in which the individual stage efficiency curves were determined for this analysis (and the magnitude of interaction effects assumed), no conclusive results can be obtained in regards to effects of interactions and first-stage performance from this case. However, at 85 percent speed (the transition speed), the small changes in performance assumed (fig. 9) indicated a computed peak efficiency of approximately 0.84 for operation with the front stage stalled and interactions in stages 2 to 4 and an efficiency of approximately 0.86 for operation with the front stage unstalled. No conclusions can be drawn at the lowest speeds considered, because no changes in stage curves were assumed for very low flow coefficients. It is obvious, however, that decreases in stage efficiency due to stall and interactions cause decreases in over-all compressor efficiency.

Case III

In order to evaluate more serious interaction effects, calculations were made for case III that assumed the same conditions in stages 1 to 4

as were assumed for case II and, in addition, assumed large interaction effects in stages 5 to 8. The modified performance curves for these middle stages are given in figure 11. The efficiencies for these stages were determined in the same manner as for the modifications in stages 1 to 4 (case II), but the magnitude of discontinuity of pressure coefficient was taken as representative of the instigation of complete total-span stall. When rotating stall existed in stage 1, stages 5 to 8 were assumed to operate on the dashed curves of figure 11. The performance of all other stages was identical to that of the previous case.

The performance of this case for the condition of unstalled operation of the inlet stage is identical to that for the previous case (fig. 10(a)). For the condition of stall of the inlet stage, however, the performance is markedly changed (fig. 12(a)).

Complete performance map. - The complete computed compressor performance map for case III is obtained by superimposing figures 10(a) and 12(a), and the resultant map is presented in figure 12(b). As in case II, the multiple performance curves at speeds above 80 percent of the reference value indicate the necessity of varying the mode of testing in component rating so that all possible compressor operating conditions can be evaluated.

Transition from stalled to unstalled operation of inlet stage. - For case III, if compressor speed is increased along the exit-vane choke limit, inlet stage unstalling will be effected at 94 percent of the reference speed. At this speed the transient change in pressure ratio would be from 4.85 to 5.2, the change in specific weight flow would be from 28.3 to 30.9, and the change in efficiency from 0.71 to 0.81. Thus, for large interaction effects, unstalling of the inlet stage is accompanied by large increases in weight flow, pressure ratio, and efficiency. The transition speed of 94 percent is shown on figure 12(b) for both the condition of stall in the inlet stage and interactions in stages 2 to 8 and the condition of no stall in the inlet stage and no interactions.

It can be seen from figure 12(b) that if interaction effects of the magnitude assumed for this case do exist and if the compressor operating characteristic follows a throttling line close to the surge limit line, unstalling of the inlet stage may not be achieved even at design speed. This phenomenon has been observed for a prototype high-pressure-ratio multistage axial-flow compressor, which was tested at this laboratory. As discussed previously, however, this situation may be relieved somewhat by compromise of the matching of the inlet stages to favor part-speed operation.

Surge limit. - The surge limit for case III exhibits a large discontinuity at 94 percent of reference speed, when normal component-rating techniques are assumed. By proper variation of speed and throttle

setting, surge may be obtained at the low-flow limit of the performance characteristics indicated by the dashed lines for speeds slightly higher than the reference value (fig. 12(b)). By increasing the speed to a value above that for unstalling of the inlet stage and then decreasing the speed, surge along the inlet stall line might be obtained down to speeds of approximately 80 percent of the reference value.

Effect of unstalling hysteresis. - If the hysteresis effect on unstalling of the inlet stage were neglected, the first stage in this case would become unstalled at 91.5 percent of reference speed for operation along the exit-vane choke limit. The general trend of performance and surge limit would, however, be unchanged. The effect of inlet-stage unstalling hysteresis is to increase the speed at which the inlet stage becomes unstalled, regardless of the throttling or compressor operating line.

Part-speed efficiency. - As can be seen from a comparison of figures 6 and 12(a), interactions of the magnitude assumed for case III result in large reductions in efficiency for operation with stall in the inlet stages. The computed values indicate a reduction of efficiency on the order of 15 percent as compared with about 2 percent for case II. Thus, the low part-speed efficiencies exhibited by some multistage axial-flow compressors may result from severe interaction effects and may be expected to exist in compressors that exhibit poor intermediate-speed surge-limit characteristics.

CONCLUDING REMARKS

The analysis reported herein has been made to study possible sources of poor part-speed efficiency and of the intermediate-speed surge problem of high-pressure-ratio multistage axial-flow compressors. Because of the simplifying assumptions used, the results obtained represent only a first approximation. The qualitative results, however, are generally in agreement with trends observed experimentally.

This analysis indicates that multiple-valued multistage performance curves will be obtained if stall of the inlet stage results in discontinuities of that stage or of one or more of the succeeding stages. Discontinuities of these succeeding stages may be a result of interaction effects due to maldistribution of flow or of nonsteady flow initiated by the first stage. The particular operating point of the compressor at the speeds where multiple curves exist is dependent on the manner in which that operating point is approached. It is believed that the dip obtained in the experimentally determined surge-limit lines of high-pressure-ratio axial-flow compressors is merely a result of transition from compressor operation with the front stages stalled to operation with these stages unstalled and that the intermediate-speed surge limit obtained by normal

3024

component test techniques may not be representative of that obtained in an engine at the same speed. Furthermore, the engine surge limit obtained during accelerations may be different from that obtained during decelerations. In order to evaluate the intermediate-speed compressor performance completely, it is recommended that operating conditions be set by both increases and decreases in speed at fixed throttle settings as well as by throttle adjustment at a fixed speed.

This analysis also indicates that extremely poor part-speed efficiencies may to a large extent be attributed to stage interactions or deterioration of stage performance due to rotating stall or maldistribution of flow imposed by the inlet stages. The magnitude of interaction effects on each stage and the number of stages affected will determine the reductions in performance at low and intermediate speeds.

Hysteresis effects in the unstalling characteristics of the first stage do not effect the existence of double-valued performance curves at intermediate speeds nor do they effect reductions in efficiency at low speeds, when discontinuities in front-stage characteristics exist because of either the type of stage stall or interactions. The existence of large unstalling hysteresis in combination with severe discontinuities in stage performance may prevent unstalling of the inlet stages until very high speeds are attained. In fact, unstalling may not even be obtained at design speed, particularly if the operating line is close to the compressor surge-limit line.

This analysis, as well as limited experimental observations, indicates that stages with continuous characteristics at their stall points are desirable from the part-speed efficiency and intermediate-speed surge aspect. "Soft stall" stages of this type generally have a progressive or partial-span stall, which originates at one end of the blade and gradually increases in severity as the flow coefficient is decreased. It should be noted that stages which have partial span or soft stall when tested as single stages may exhibit discontinuities when operating in a multistage compressor at off-design conditions of speed and flow.

More complete data are required on effects of stage design and blading geometry on stage stall characteristics as well as effects of stage interactions due to radial maldistribution of flow and nonsteady flow as encountered in multistage compressors. In addition, this analysis indicates the need for a more complete evaluation of compressor performance and surge limits in the intermediate-speed range.

Lewis Flight Propulsion Laboratory
National Advisory Committee for Aeronautics
Cleveland, Ohio, September 17, 1953

CONFIDENTIAL

APPENDIX A

SYMBOLS

The following symbols are used in this report:

A	area, sq ft
c_p	specific heat at constant pressure, Btu/lb/°F
g	acceleration due to gravity, 32.17 ft/sec ²
H	enthalpy, ft-lb/slug
J	mechanical equivalent of heat, 778.3 ft-lb/Btu
P	stagnation pressure, lb/sq ft
R	gas constant, ft-lb/lb °F
r	radius, ft
T	stagnation temperature, °R
U	wheel speed, ft/sec
V	velocity, ft/sec
W	weight-flow rate, lb/sec
$\frac{W\sqrt{\theta}}{\delta}$	equivalent flow rate, lb/sec
Y	$\left(\frac{P_2}{P_1}\right)^{\frac{\gamma-1}{\gamma}} - 1$
β	flow angle measured from axial direction, deg
γ	ratio of specific heats, 1.40
δ	ratio of pressure to standard pressure
η	adiabatic efficiency
θ	ratio of temperature to standard temperature

ρ density, slugs/cu ft

ϕ flow coefficient, $\left(\frac{V_a}{U_m}\right)$

ψ pressure coefficient, $\frac{gJc_p T_{st} Y}{\left(\frac{U_m}{\sqrt{\theta}}\right)^2}$

Subscripts:

1 inlet to first stage

2 exit of first stage or inlet to second stage

a axial component

ac actual

is isentropic

m mean radius (average of tip speed and root radii)

s static

st standard

t total

APPENDIX B

CALCULATIONS OF OFF-DESIGN PERFORMANCE OF MULTISTAGE

AXIAL-FLOW COMPRESSORS

The design, fabrication, and testing of multistage axial-flow compressors in order to evaluate the effects of changes in design variables is an extremely costly and time-consuming process. In addition, compressor surge and stage interactions limit the attainment of data in the range of compressor stall. Therefore, a one-dimensional technique of stage stacking has been used to formulate multistage compressor performance maps from representative stage performance data and thus obtain generalized trends of internal-flow characteristics at off-design operating conditions. The absolute values of compressor performance obtained by this method are only qualitative, inasmuch as simplifying assumptions are required. The trends obtained, however, are extremely valuable in a study of off-design performance.

For simplicity of calculation, the individual stage data for all speeds are correlated on the basis of pressure coefficient ψ and adiabatic efficiency η against a flow coefficient φ . These coefficients are expressed as follows:

$$\psi = \frac{\Delta H_{1s}/\theta}{\left(\frac{U_m}{\sqrt{\theta}}\right)^2} = \frac{gJc_p T_{st} Y}{\left(\frac{U_m}{\sqrt{\theta}}\right)^2} = f_1(\varphi) \quad (B1)$$

$$\eta = \frac{\Delta H_{1s}}{\Delta H_{ac}} = f_2(\varphi) \quad (B2)$$

$$\varphi = \left(\frac{V_a}{U}\right)_m \quad (B3)$$

Correlation of stage performance on the basis of the preceding parameters neglects the effects of compressibility and Reynolds number on the stage efficiency and flow range, and the radial distribution of flow geometry is assumed to be defined by the mean radius ratio of axial velocity to wheel speed. This method therefore ignores the effects of radial maldistribution of inlet velocity on stage performance. Correlation of stage data from both single-stage and multistage compressors have shown this correlation to be satisfactory over a wide range of speeds and Mach numbers. The correlation does give some scatter of data when Mach numbers exceed 0.75 or when stage pressure ratios greatly exceed those commonly used for axial-flow compressors.

The first step in the stacking procedure is to select the generalized stage characteristics for each stage in terms of pressure coefficient and adiabatic stage efficiency as functions of flow coefficient. The second step is to determine the area ratio through the compressor so that all stages operate at the desired value of flow coefficient at the design or reference value of inlet flow and rotative speed. A compressor map is then determined by stage-to-stage calculation for several values of inlet flow at each rotative speed to be considered.

The flow coefficient into the first stage is determined from the conventional weight-flow parameter $W\sqrt{\theta_1}/\delta_1$, the rotative speed $U_{m,1}/\sqrt{\theta_1}$, and the effective stage inlet area.

From continuity,

$$V_{a,1} = \frac{W}{\rho_{s,1} A_1}$$

or

$$\frac{V_{a,1}}{\sqrt{\theta_1}} = \frac{W\sqrt{\theta_1} T_{st} P_1}{\delta_1 A_1 T_1 P_{st} \rho_{s,1}} \quad (B4)$$

By combining equation (B4) with the perfect gas law

$$\frac{P_1}{T_1} = g R \rho_{t,1} \quad (B5)$$

with the expression

$$\frac{\rho_{s,1}}{\rho_{t,1}} = \left(1 - \frac{V_1^2}{2gJc_p T_1} \right)^{\frac{1}{\gamma-1}} \quad (B6)$$

and with the vector diagram relation

$$V_1 = \frac{V_{a,1}}{\cos \beta_1} \quad (B7)$$

the following equation is obtained:

$$\frac{W\sqrt{\theta_1}}{\delta_1 A_1} = \left(\frac{V_{a,1}}{\sqrt{\theta_1}} \right) \left[1 - \left(\frac{V_{a,1}}{\sqrt{\theta_1}} \right)^2 \frac{1}{2gJc_p T_{st} \cos^2 \beta_1} \right]^{\frac{1}{\gamma-1}} g p_{st} \quad (B8)$$

The solution of equation (B8) can most readily be obtained by computing values of $W\sqrt{\theta}/\delta A$ for various values of $V_a/\sqrt{\theta}$ and an assigned value of β . The flow coefficient is then determined from the equation

$$\varphi_1 = \frac{\frac{V_{a,1}}{\sqrt{\theta_1}}}{\frac{U_{m,1}}{\sqrt{\theta_1}}} \quad (B9)$$

After the flow coefficient is determined, the values of pressure coefficient and adiabatic efficiency are obtained from the generalized stage performance curves. The stage pressure ratio is obtained from the pressure coefficients ψ as follows:

$$\frac{P_2}{P_1} = \left[1 + \frac{\psi_1 \left(\frac{U_{m,1}}{\sqrt{\theta_1}} \right)^2}{gJc_p T_{st}} \right]^{\frac{\gamma}{\gamma-1}} \quad (B10)$$

and the stage temperature ratio, from the pressure coefficient and adiabatic efficiency:

$$\frac{T_2}{T_1} = \left[1 + \frac{\psi_1 \left(\frac{U_m}{\sqrt{\theta}} \right)^2}{\eta_1 gJc_p T_{st}} \right] \quad (B11)$$

The weight-flow parameter for the second stage $W\sqrt{\theta_2}/\delta_2 A_2$ is determined from the parameter for stage 1 by the expression

$$\frac{W\sqrt{\theta_2}}{\delta_2 A_2} = \frac{W\sqrt{\theta_1}}{\delta_1 A_1} \frac{A_1}{A_2} \frac{\sqrt{\frac{T_2}{T_1}}}{\frac{P_2}{P_1}} \quad (B12)$$

and the rotative speed $U_{m,2}/\sqrt{\theta_2}$ is determined by the expression

$$\frac{U_{m,2}}{\sqrt{\theta_2}} = \frac{U_{m,1}}{\sqrt{\theta_1}} \frac{\left(\frac{r_{m,2}}{r_{m,1}}\right)}{\sqrt{\frac{T_2}{T_1}}} \quad (B13)$$

The flow coefficient is

$$\phi_2 = \frac{\frac{V_{a,2}}{\sqrt{\theta_2}}}{\frac{U_{m,2}}{\sqrt{\theta_2}}} \quad (B14)$$

In the design or reference-point phase of the calculation, the flow coefficient for the second stage is selected, and the area ratio and radius ratio must be so determined as to give the desired value of ϕ_2 . The area ratio A_2/A_1 and the radius ratio $r_{m,2}/r_{m,1}$ are related by the type of design, that is, constant tip diameter, constant pitch diameter, or constant root diameter. For the design computed herein, a constant tip diameter was used, and the area ratio was determined by a trial-and-error process. For off-design performance calculations, the area ratio and radius ratio are known and the flow coefficient is computed directly. The pressure ratio and temperature ratio for the second stage are then computed the same as for stage 1.

The preceding process is then repeated for each stage throughout the compressor. Over-all pressure ratio and temperature ratio are taken as the product of the stage values, and the over-all adiabatic efficiency is computed from over-all temperatures and pressures. For off-design performance calculations, inlet weight flows must be properly chosen so that all stages remain within the limits of their individual flow ranges.

For conditions where the stage pressure ratios are less than 1.00, plots of ψ and ψ/η against ϕ were used to compute stage pressure ratio and temperature ratio.

REFERENCES

1. Huppert, Merle C.: Preliminary Investigation of Flow Fluctuations During Surge and Blade Row Stall in Axial-Flow Compressors. NACA RM E52E28, 1952.

~~CONFIDENTIAL~~

2. Huppert, Merle C., Costilow, Eleanor L., and Budinger, Ray E.: Investigation of a 10-Stage Subsonic Axial-Flow Research Compressor. III - Investigation of Rotating Stall, Blade Vibration, and Surge at Low and Intermediate Compressor Speeds. NACA RM E53C19, 1953.
3. Grant, Howard P.: Hot Wire Measurements of Stall Propagation and Pulsating Flow in an Axial Flow Inducer-Centrifugal Impeller System. Pratt and Whitney Res. Rep. No. 133, June 1951.
4. Iura, T., and Rannie, W. D.: Observations of Propagating Stall in Axial-Flow Compressors. Rep. No. 4, Mech. Eng. Lab., C.I.T., Apr. 1953. (Navy Contract N6-ORI-102, Task Order 4.)
5. Medeiros, Arthur A., Benser, William A., and Hatch, James E.: Analysis of Off-Design Performance of a 16-Stage Axial-Flow Compressor with Various Blade Modifications. NACA RM E52L03, 1953.
6. Huppert, Merle C., and Benser, William A.: Some Stall and Surge Phenomena in Axial-Flow Compressors. Paper presented at Twenty-First Inst. Aero. Sci. meeting, New York (N. Y.), Jan. 26-29, 1953.
7. Burtt, Jack R.: Investigation of Performance of Typical Inlet Stage of Multistage Axial-Flow Compressor. NACA RM E9E13, 1949.
8. Jackson, Robert J.: Effects on the Weight-Flow Range and Efficiency of a Typical Axial-Flow Compressor Inlet Stage that Result from the Use of a Decreased Blade Camber or Decreased Guide-Vane Turning. NACA RM E52G02, 1952.
9. Huppert, Merle C., Johnson, Donald F., and Costilow, Eleanor L.: Preliminary Investigation of Compressor Blade Vibration Excited by Rotating Stall. NACA RM E52J15, 1952.
10. Graham, Robert W., and Prian, Vasily D.: Experimental and Theoretical Investigation of Rotating-Stall Characteristics of Single-Stage Axial-Flow Compressor with Hub-Tip Ratio of 0.76. NACA RM E53I09, 1953.
11. Finger, Harold B., and Dugan James F., Jr.: Analysis of Stage Matching and Off-Design Performance of Multistage Axial-Flow Compressors. NACA RM E52D07, 1952.
12. Foster, D. V.: The Performance of the 108 Compressor Fitted with Low Stagger Free Vortex Blading. Rep. No. R.116, British N.G.T.E., June 1952.

3024

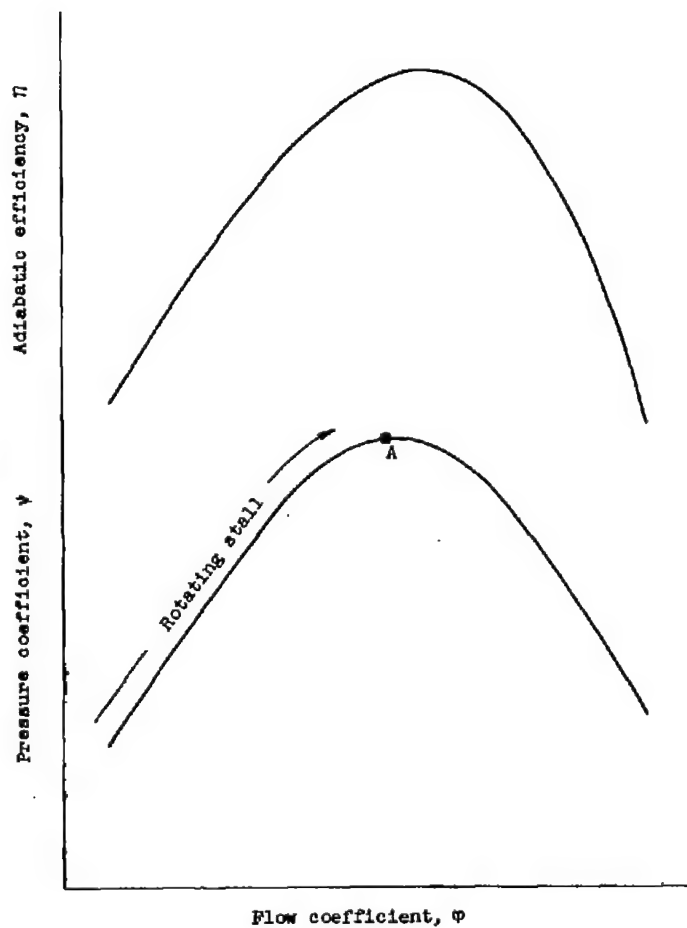
~~CONFIDENTIAL~~

TABLE I. - TABULATION OF REFERENCE-POINT VALUE

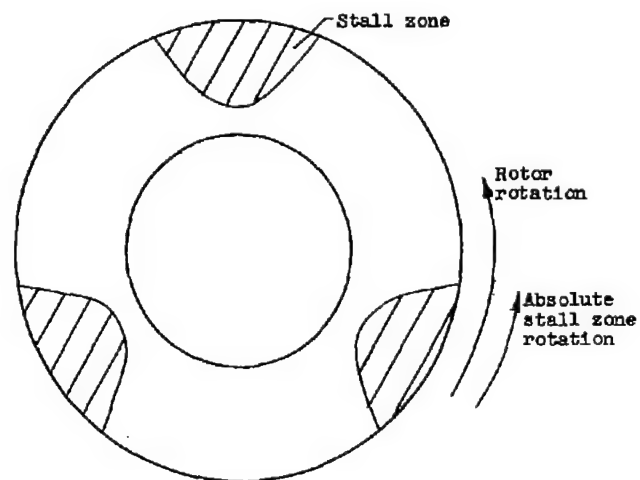
Stage	Area ratio ¹	Mean radius ratio ²	Hub-tip ratio	Stage pressure ratio
1	0.8431	1.071	0.5	1.179
2	.8510	1.046	.6063	1.196
3	.8547	1.033	.6795	1.203
4	.8580	1.025	.7348	1.204
5	.8630	1.019	.7779	1.202
6	.8695	1.015	.8120	1.198
7	.8720	1.012	.8389	1.192
8	.8780	1.010	.8613	1.186
9	.8835	1.008	.8794	1.179
10	.8875	1.007	.8943	1.172
11	.8920	1.0055	.9068	1.166
12	.8960	1.0046	.9173	1.159

¹Ratio of exit to inlet area for the stage.

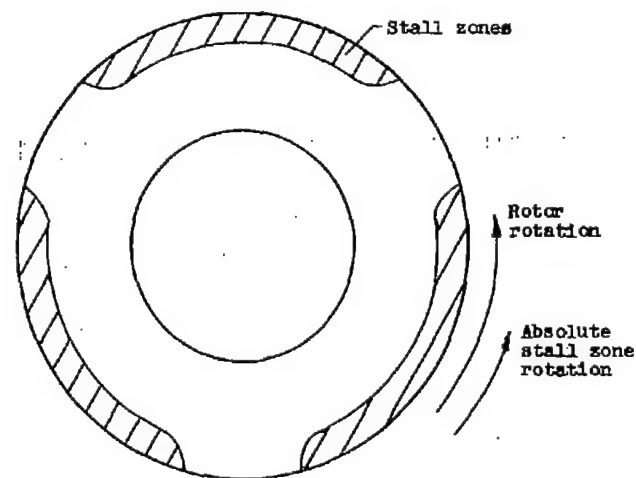
²Ratio of exit to inlet mean radius for the stage.



(a) Stage performance.

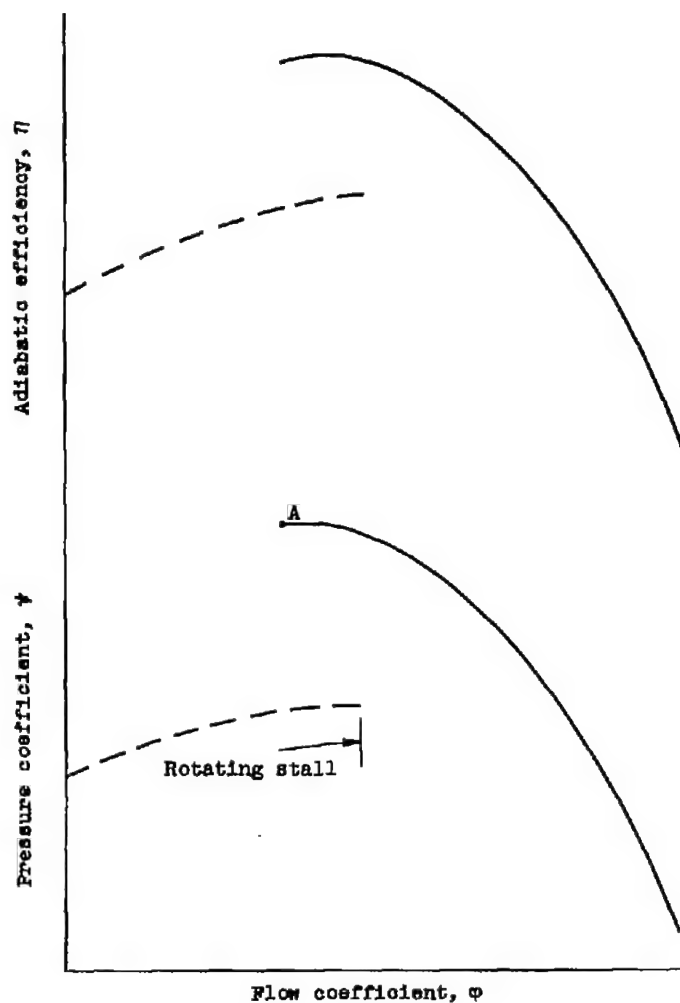


(b) Schematic cross section of annulus.

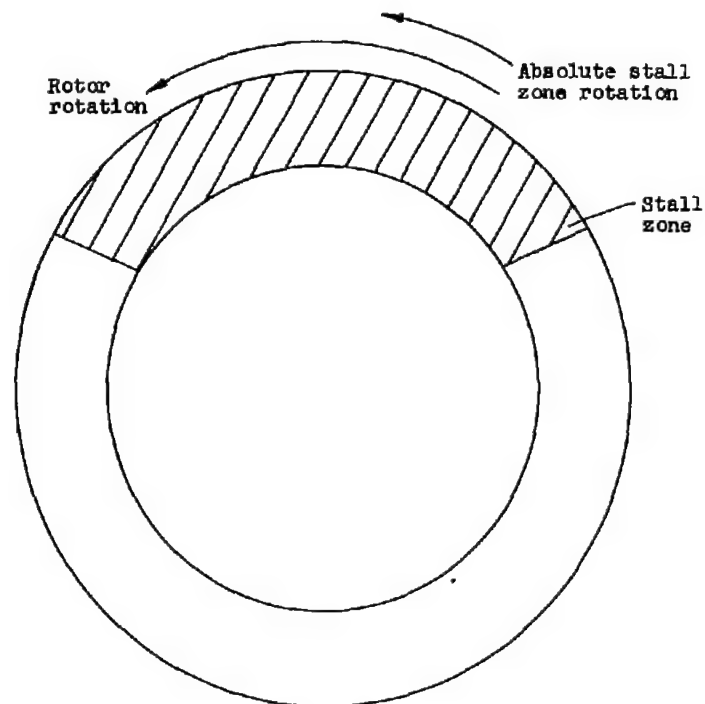


(c) Schematic cross section of annulus for blading that is extremely critical at tip.

Figure 1. - Characteristics of stage having partial-span-type rotating stall.



(a) Stage performance.



(b) Schematic cross section of annulus.

Figure 2. - Characteristics of stage having total-span-type rotating stall.

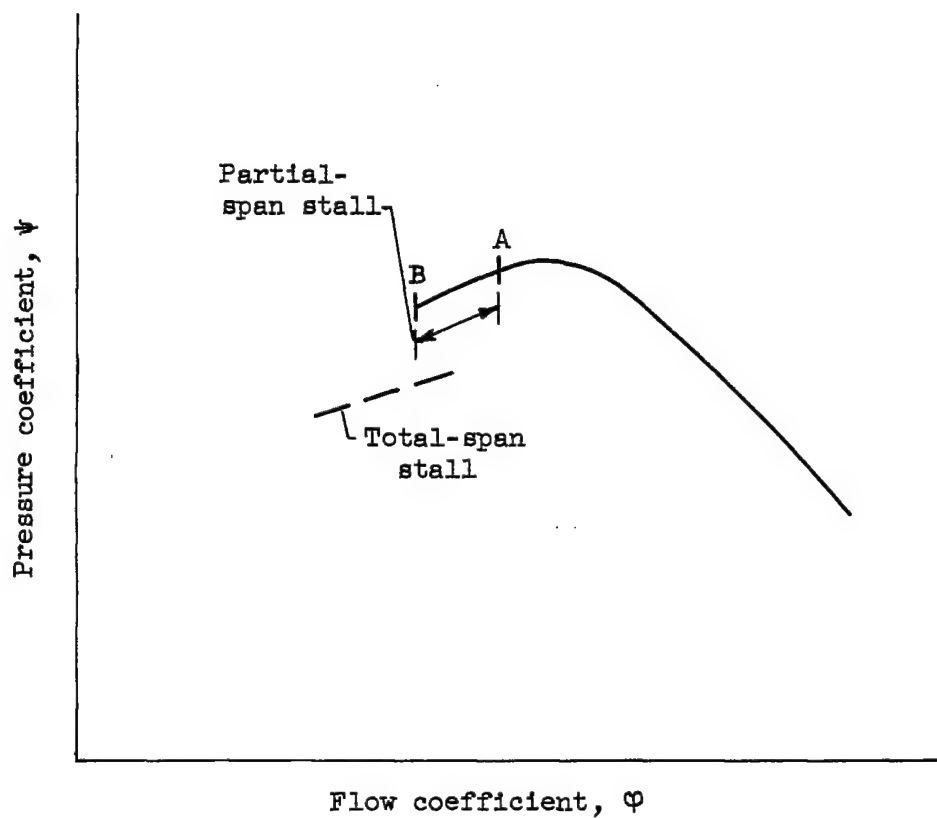


Figure 3. - Performance of intermediate hub-tip ratio stage with both partial- and total-span stall.

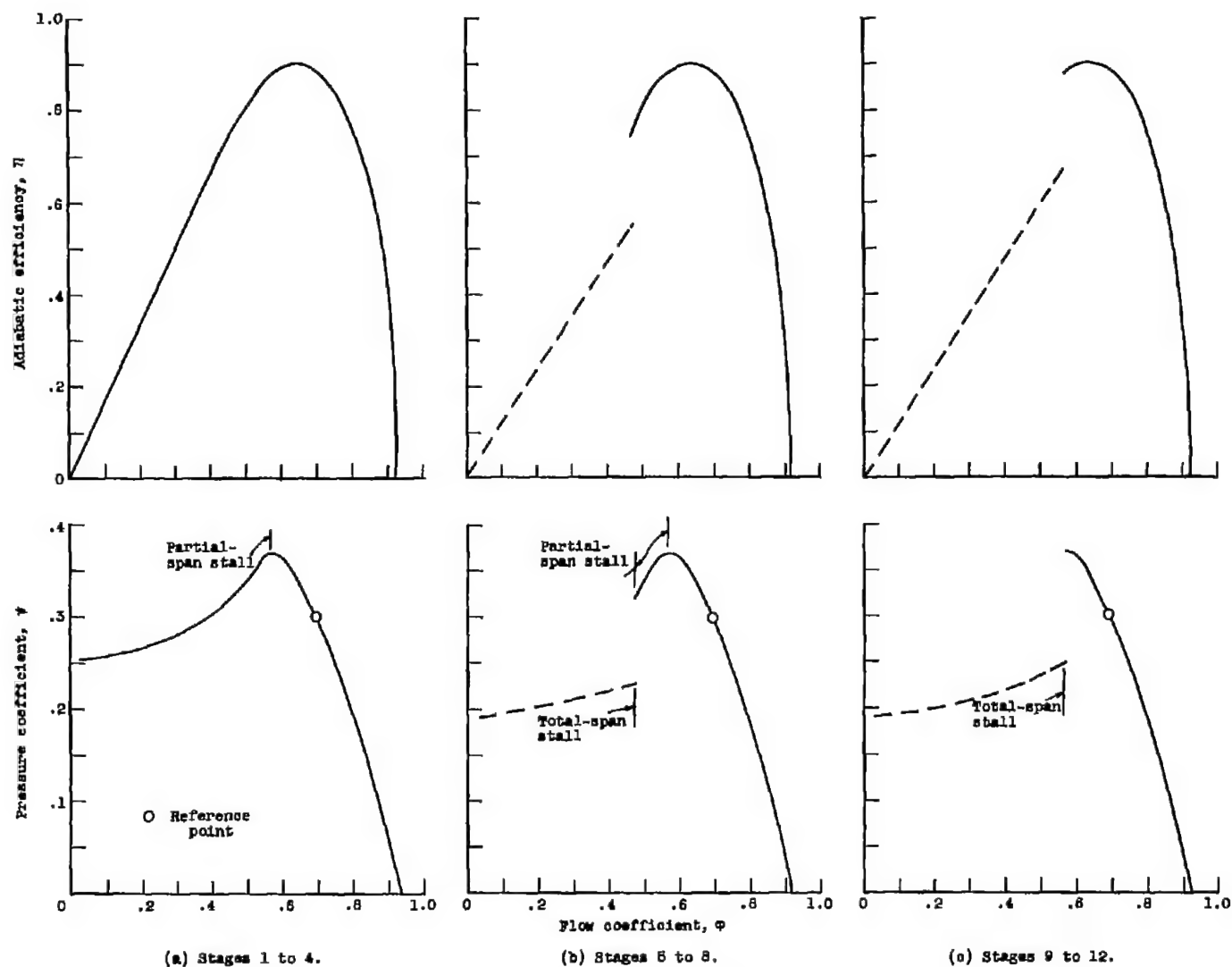


Figure 4. - Assumed stage performance characteristics for case I.

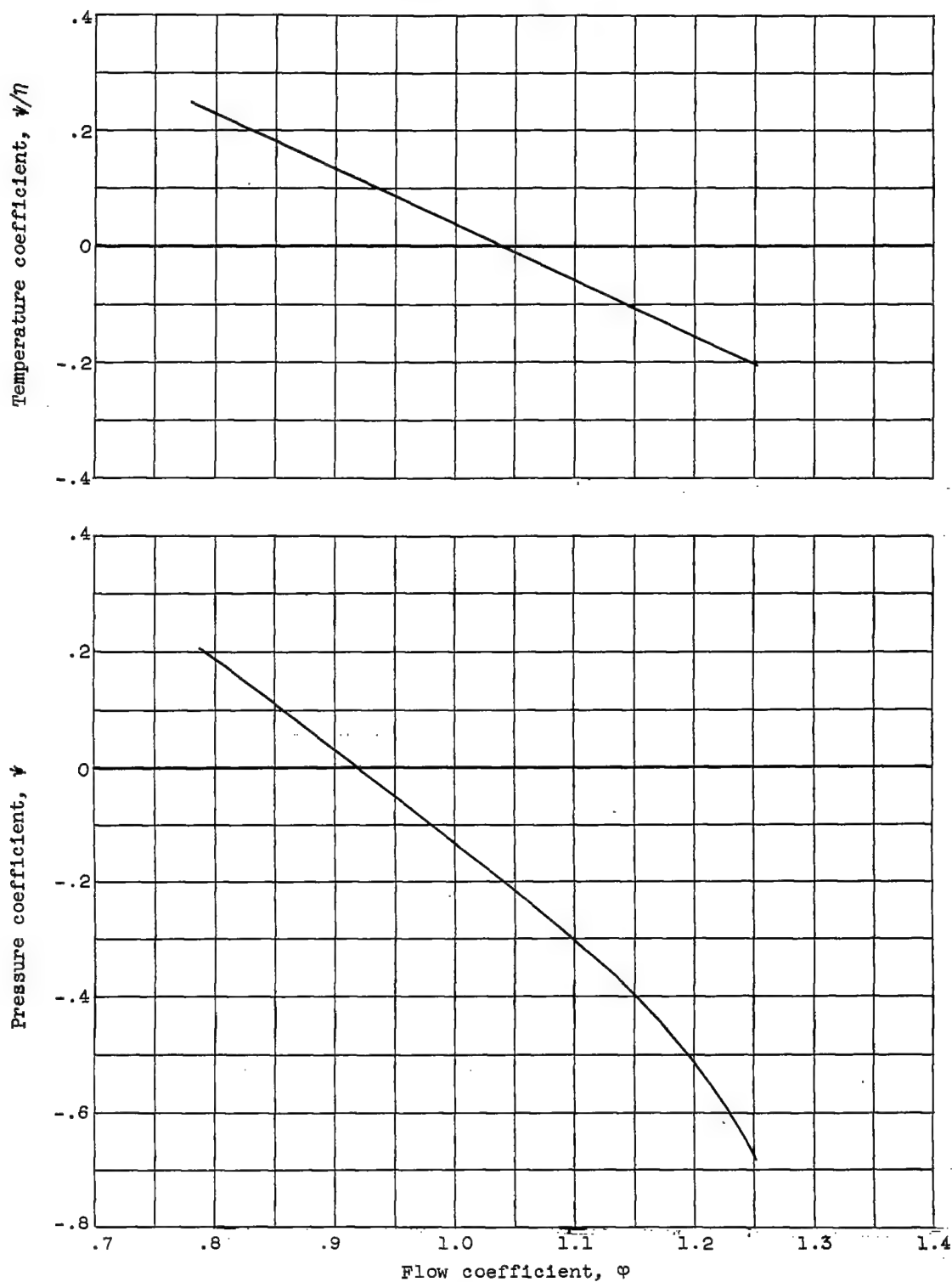


Figure 5. - Assumed performance characteristics for negative values of pressure coefficient for all stages.

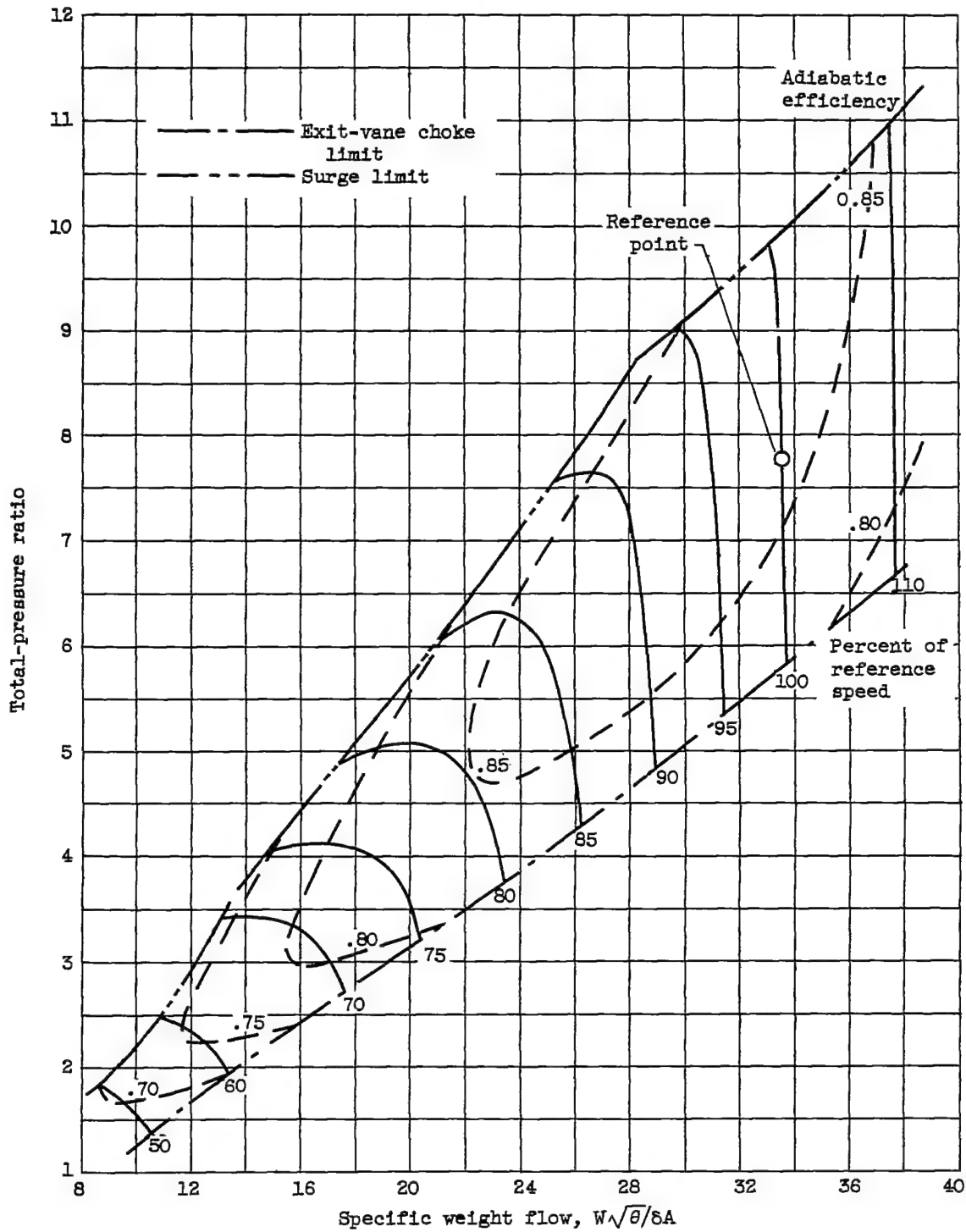


Figure 6. - Computed over-all performance for case I.

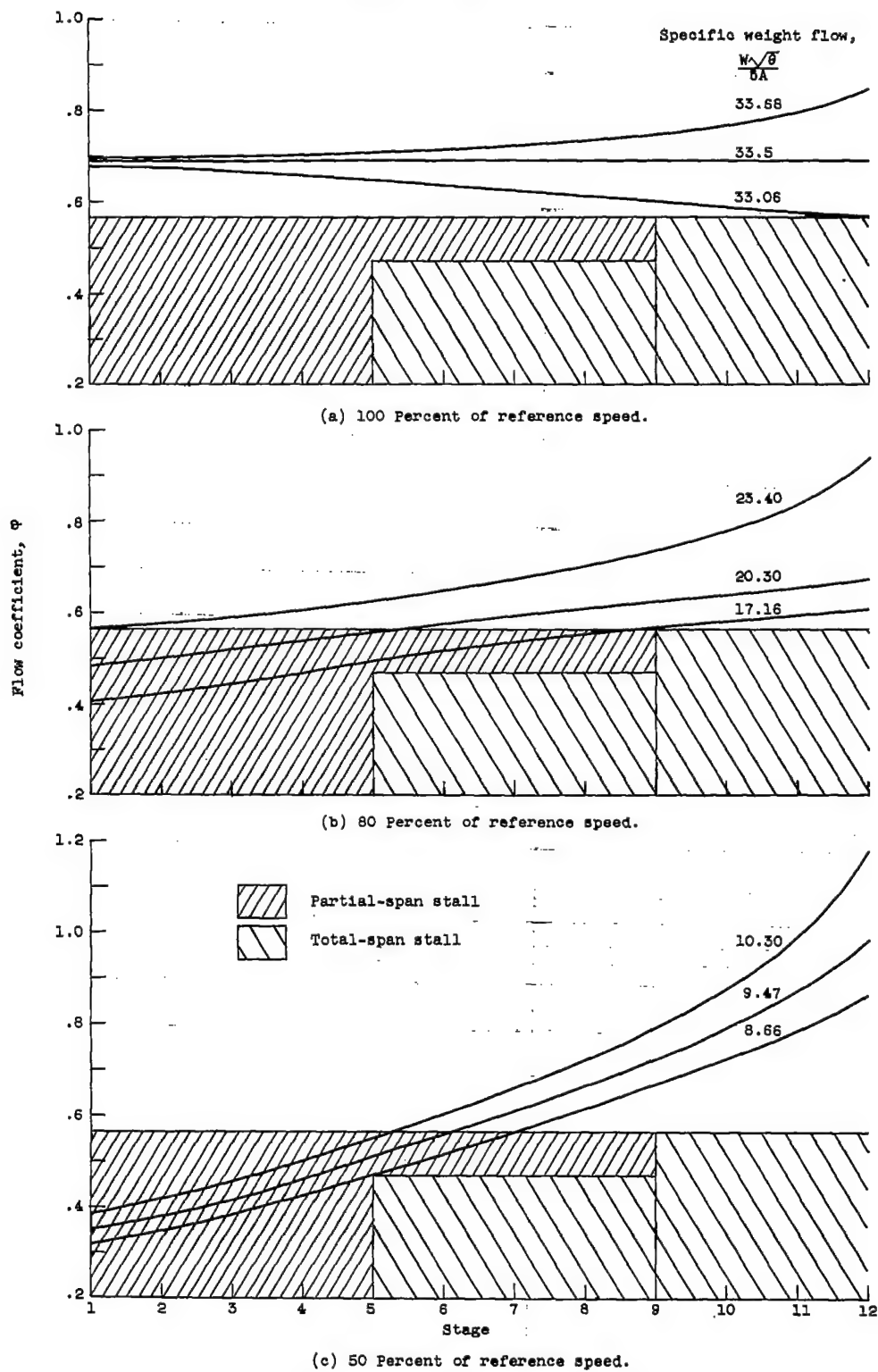


Figure 7. - Stagewise variation of flow coefficient for case I.

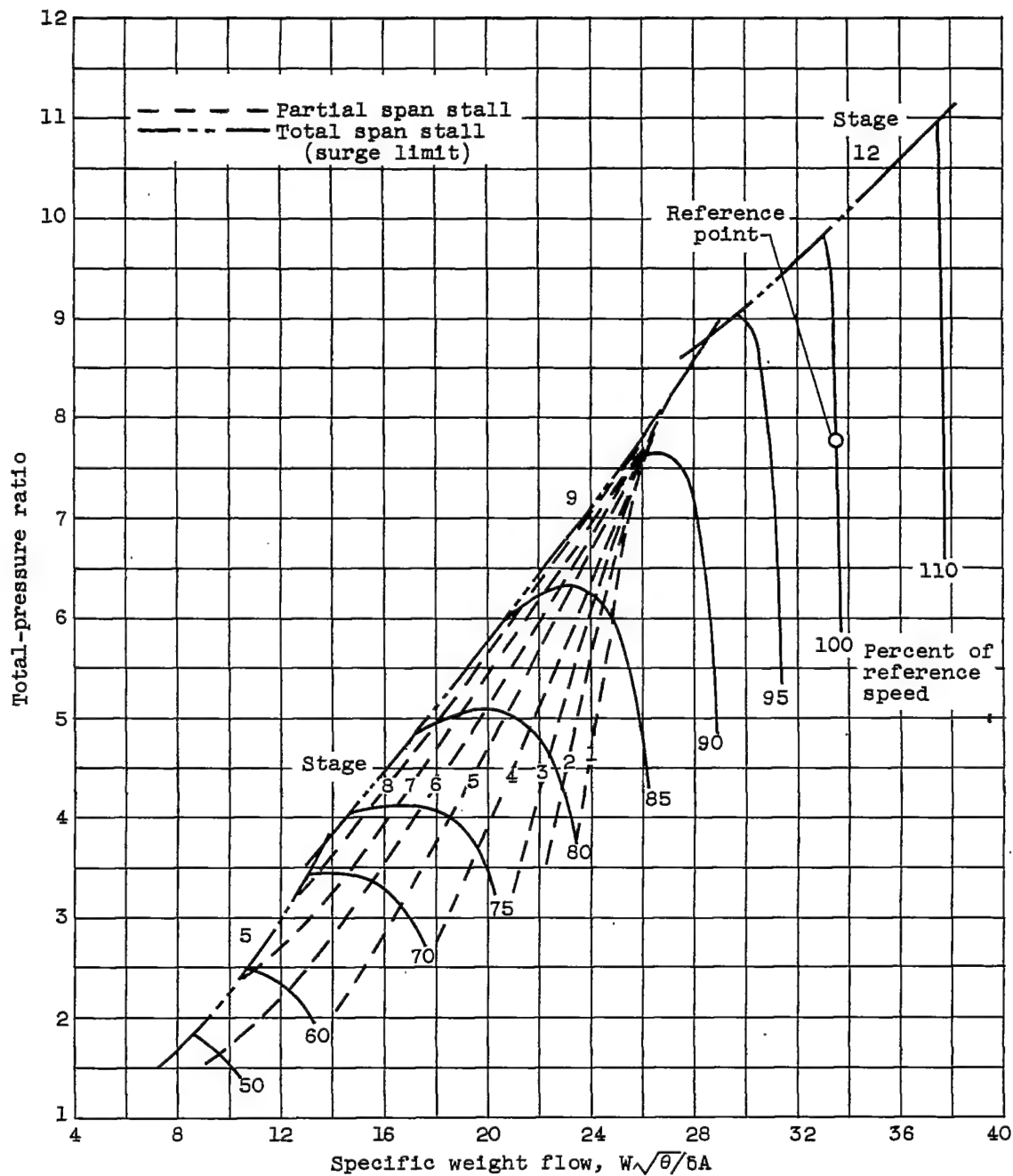


Figure 8. - Relation of stage stall and over-all compressor performance for case I.

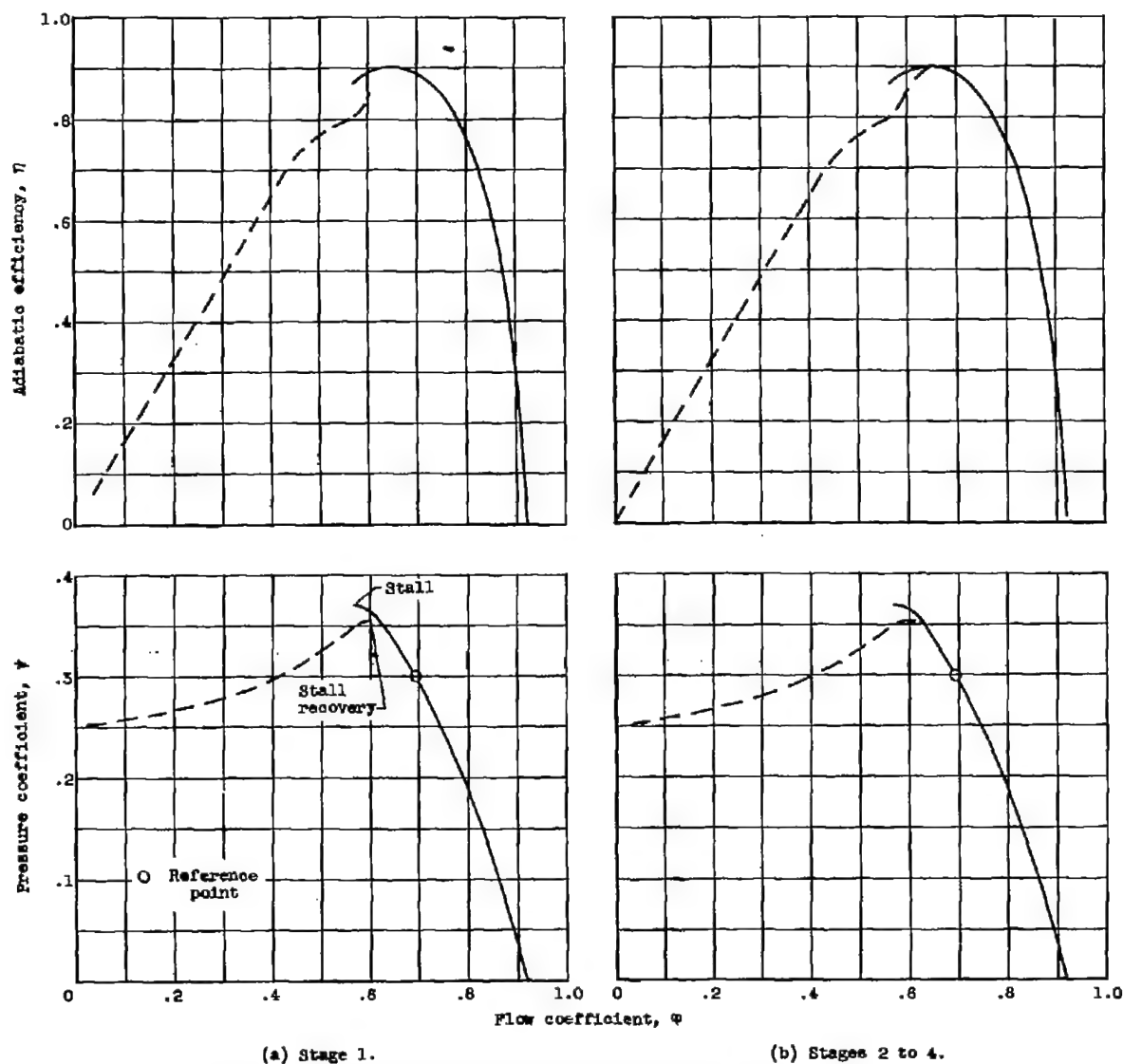
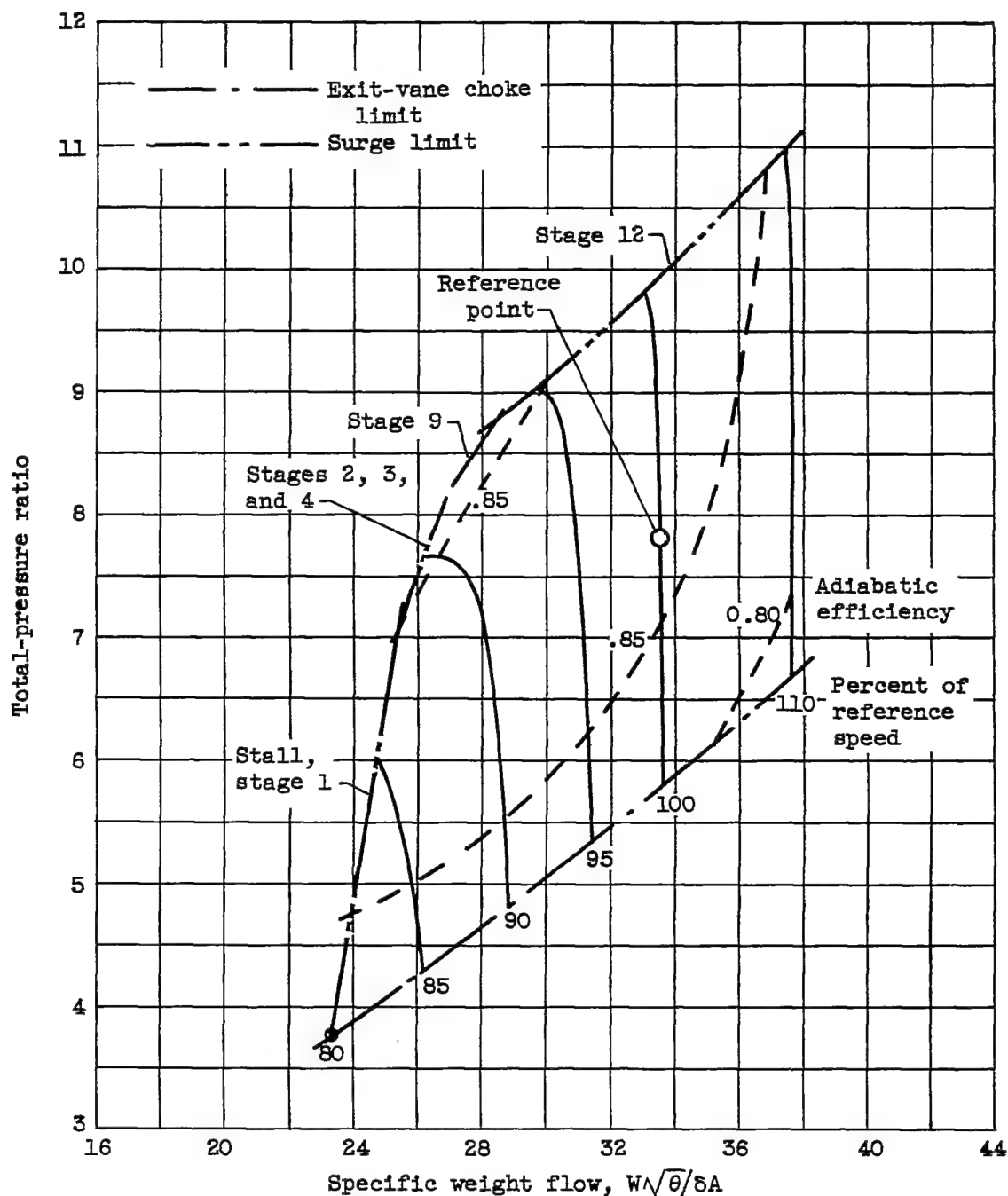
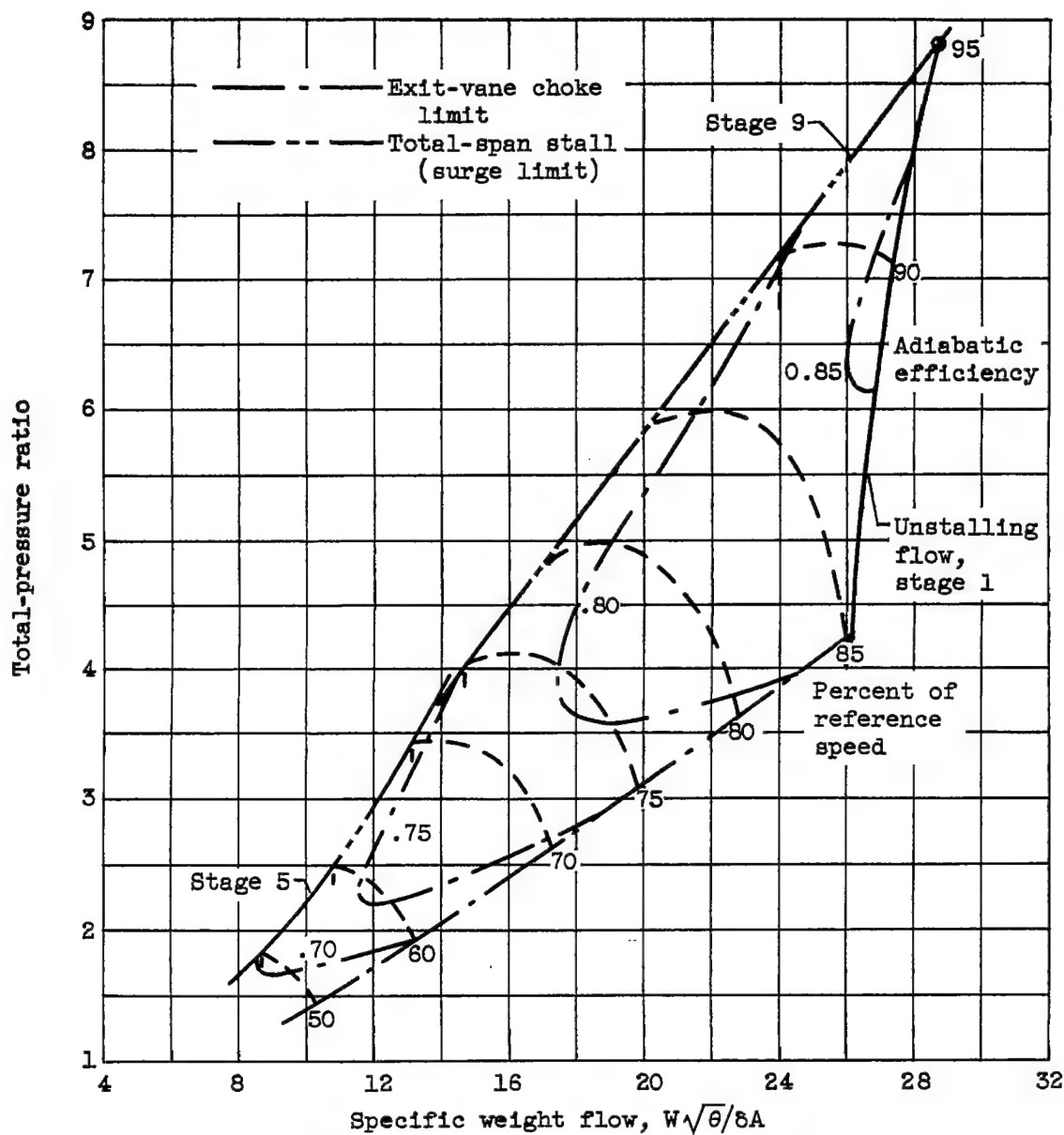


Figure 2. - Assumed performance characteristics for stages 1 to 4 for case II.



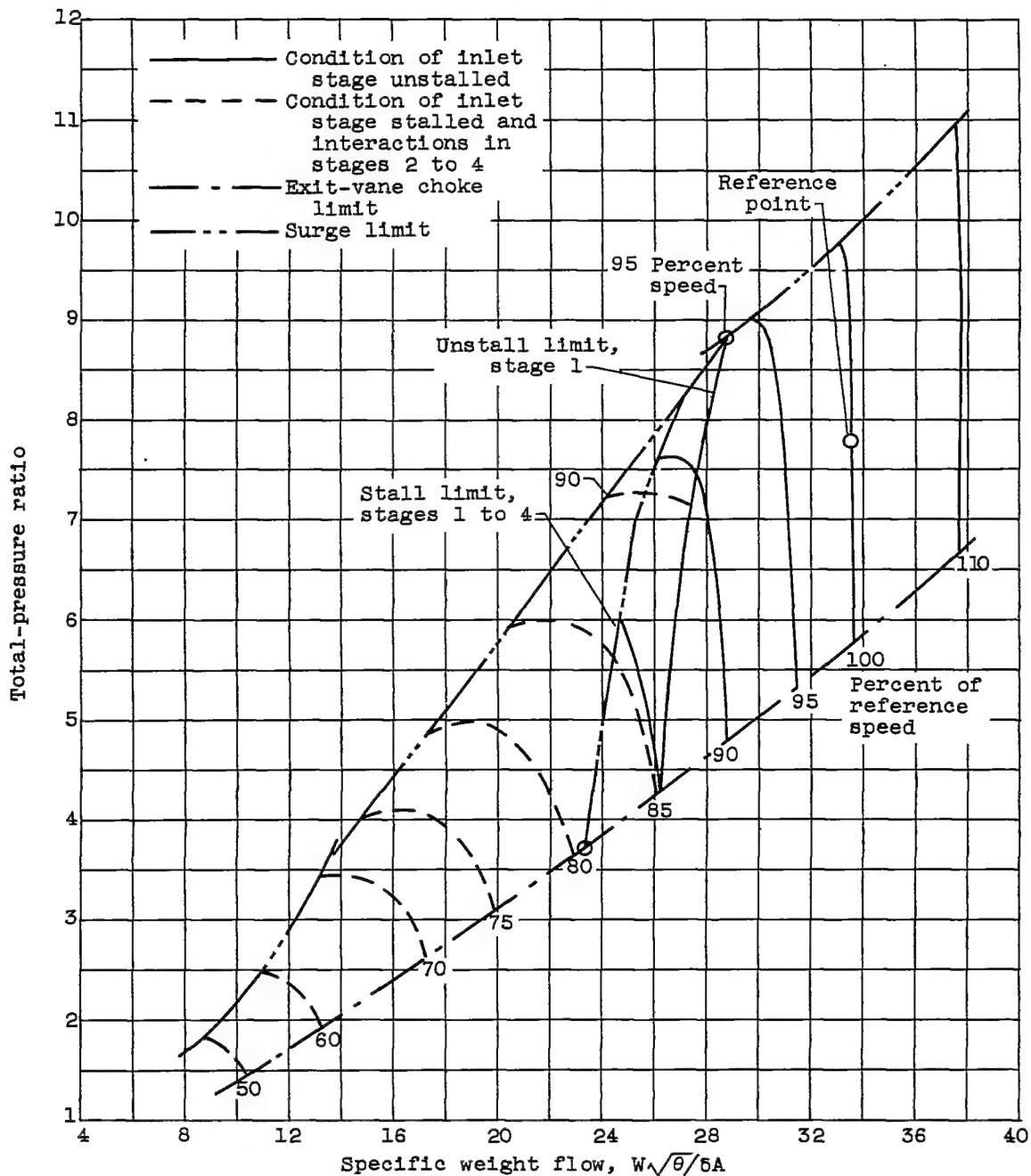
(a) Front stage unstalled.

Figure 10. - Computed over-all performance for case II.



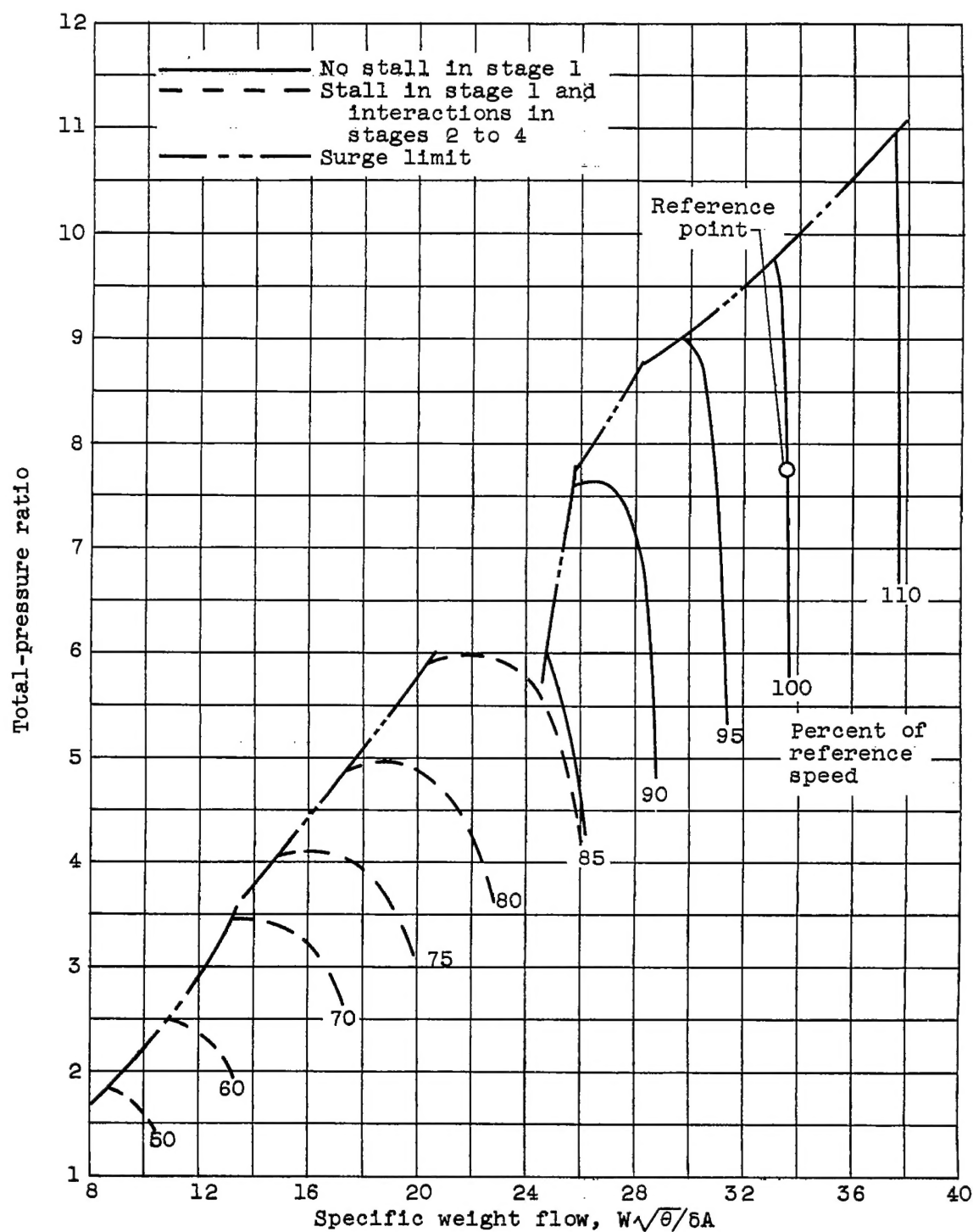
(b) Front stage stalled and interactions in stages 2 to 4.

Figure 10. - Continued. Computed over-all performance for case II.



(c) Composite performance (superposition of fig. 10(a) and 10(b)).

Figure 10. - Continued. Computed over-all performance for case II.



(d) Transition from stalled to unstalled inlet stage on exit-vane choke line.

Figure 10. - Concluded. Computed over-all performance for case II.

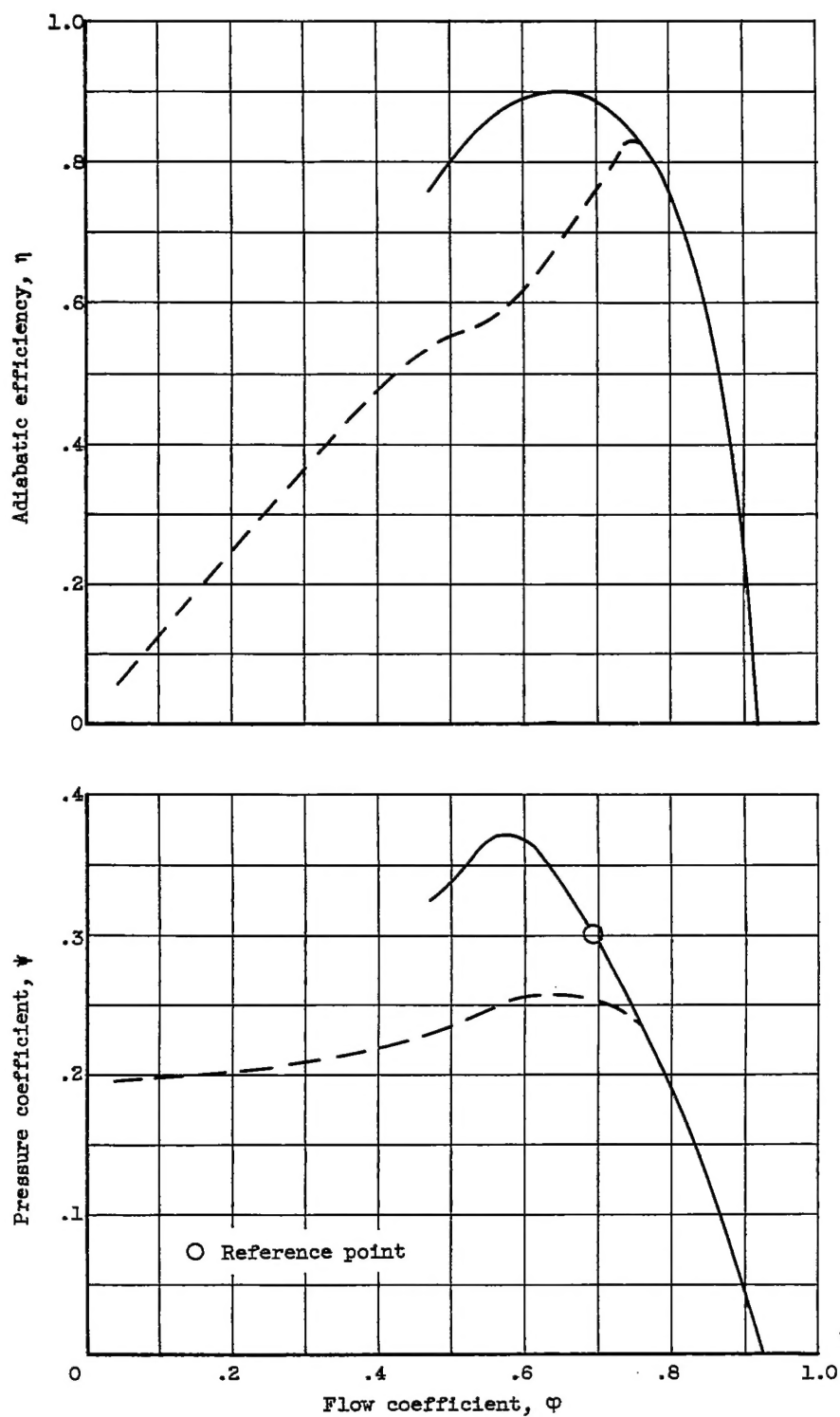
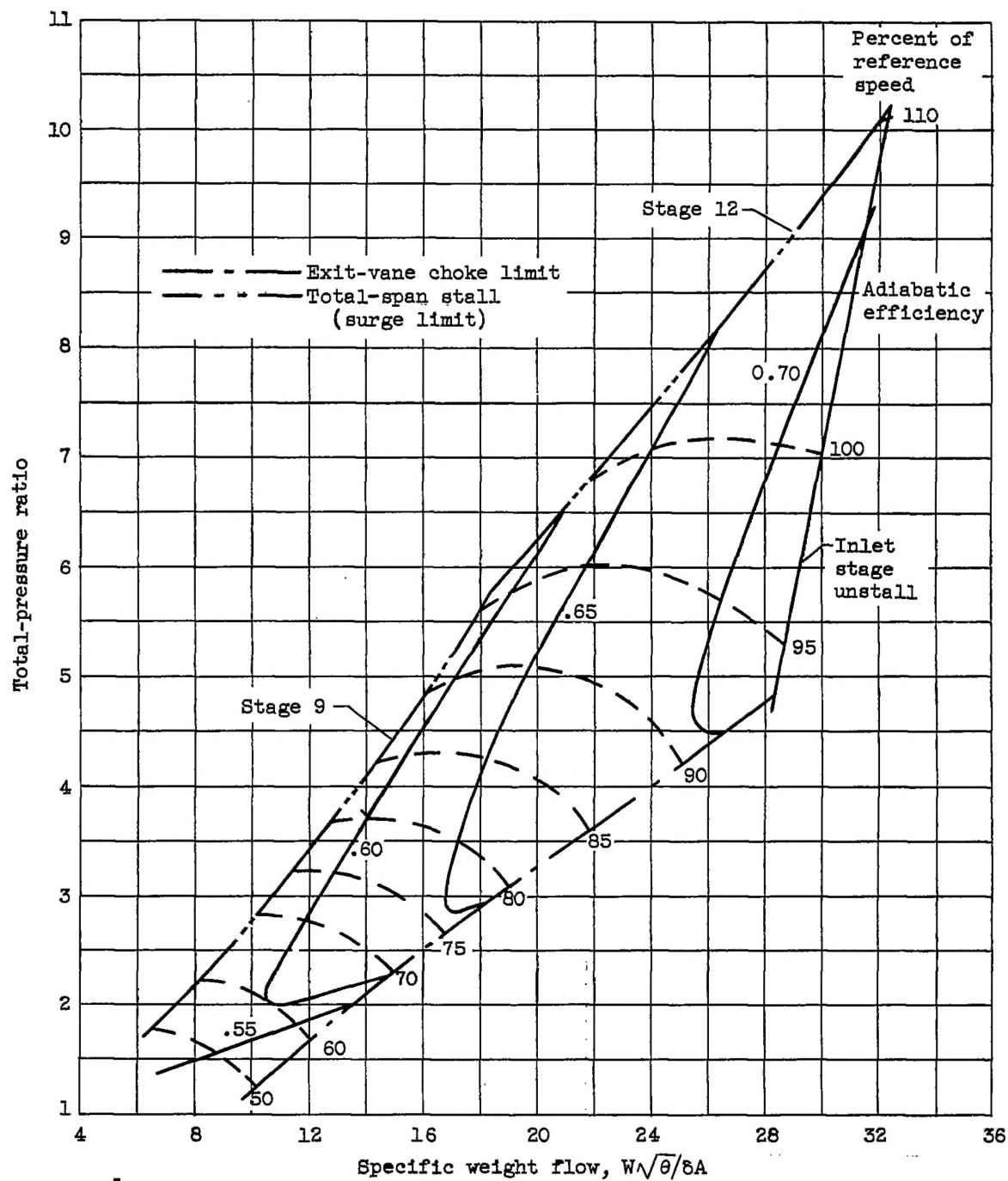
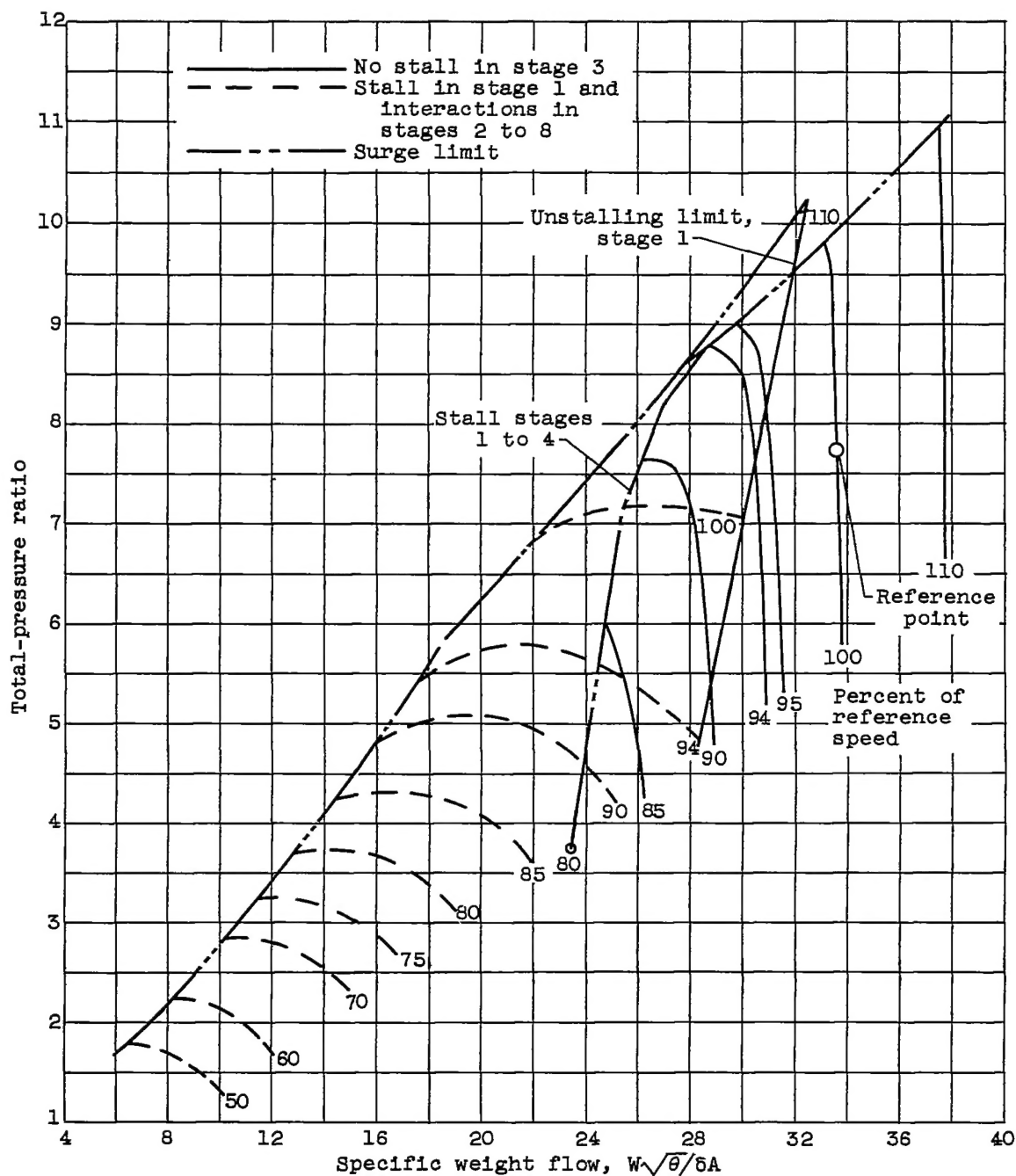


Figure 11. - Assumed performance characteristics for stages 5 to 8 for case III.



(a) Front stage stalled and interactions in stages 2 to 8.

Figure 12. - Computed over-all performance for case III.



(b) Composite performance (superposition of figs. 10(a) and 12(a)).

Figure 12. - Concluded. Computed over-all performance for case III.